controlled. Normally, the recrystallization temperature of a metal is about 40% of its melting temperature in the absolute scale but this temperature depends also on the amount of prior cold work.

Figure 1.38a shows the variation of mechanical properties with the amount of mechanical working. Apart from changing the mechanical properties, the amount of cold work also governs the recrystallized grain size (see Fig. 1.38b).

2 Casting Processes

2.1 INTRODUCTION

Casting is one of the oldest manufacturing processes, and even today is the first step in manufacturing most products. In this process, the material is first liquefied by properly heating it in a suitable furnace. Then, the liquid is poured into a previously prepared mould cavity where it is allowed to solidify. Subsequently, the product is taken out of the mould cavity, trimmed, and cleaned to shape.

It is clear from the definition of the process that a successful casting operation needs a knowledge in the following areas:

(i) Preparation of moulds and patterns (used to make the mould).

(ii) Melting and pouring of the liquefied metal.

(iii) Solidification and further cooling to room temperature.

(iv) Defects and inspection.

There are various types of casting processes depending, among others, on the material, the type of patterns and moulds, and the pouring technique. Before going into the details of these processes, we shall discuss the basic common features among the various casting processes in the context of the four areas we have just mentioned.

The suitability of the casting operation for a given material depends on

(i) the melting temperature of the job and the mould materials,

(ii) the solubility of and the chemical reaction between the job and the mould materials,

(iii) the solubility of the atmosphere in the material at different temperatures to be encountered in the casting operation,

(iv) the thermal properties such as conductivity and coefficient of linear expansion of both the mould and job materials.

2.2 PATTERN AND MOULD

A pattern is the replica of the part to be cast and is used to prepare the mould cavity. Patterns are made of either wood or metal. A mould is an assembly of two or more metal blocks, or bonded refractory particles (sand) consisting of a primary cavity. The mould cavity holds the liquid material and essentially acts as a negative of the desired product. The mould also contains secondary cavities for pouring and channeling the liquid material into the primary cavity and to act as a reservoir, if necessary.

A four-sided frame in which a sand mould is made is referred to as a *flask*. If the mould is made in more than one part, the top portion is called the *cope* and the bottom one is termed as the *drag*. For producing hollow sections, the entry of the liquid metal is prevented by having a *core* in the corresponding portion of the mould cavity. The projections on the pattern for locating the core in the mould are called *core prints*. There are diverse types of patterns and moulds depending on the material, the job, and the number of castings required.

2.2.1 PATTERN ALLOWANCES

A pattern is always made somewhat larger than the final job to be produced. This excess in dimensions is referred to as the pattern allowance. There are two categories of pattern allowances, namely, the *shrinkage allowance* and the *machining allowance*.

The shrinkage allowance is provided to take care of the contractions of a casting. The total contraction of a casting takes place in three stages, and consists of

(i) the contraction of the liquid from the pouring temperature to the freezing temperature,

(ii) the contraction associated with the change of phase from liquid to solid,

(iii) the contraction of the solid casting from the freezing temperature to the room temperature.

It must be noted, however, that it is only the *last* stage of the contraction which is taken care of by the shrinkage allowance. (The other two categories of contraction will be discussed in Section 2.5.) Obviously, the amount of shrinkage allowance depends on the linear coefficient of thermal expansion α_l of the material. The higher the value of this coefficient, the more the value of shrinkage allowance. For a dimension l of a casting, the shrinkage allowance is given by the product $\alpha_l l(\theta_f - \theta_0)$, where θ_f is the freezing point of the material and θ_0 is the room temperature. This is normally expressed per unit length for a given material. Table 2.1 gives some quantitative idea about the shrinkage allowance for casting different materials.

Usually, a cast surface is too rough to be used in the same way as the surface of the final product. As a result, machining operations are required to produce the finished surface. The excess in the dimensions of the casting (and consequently in the dimensions of the pattern) over those of the final job to take care of the machining is called the machining allowance. The total machining allowance also depends on the material and the overall dimension of the job, though not linearly as the shrinkage allowance. Table 2.1 gives also an idea of the machining allowance for various materials. For internal surfaces, the allowances provided should obviously be negative, and normally the machining allowances are 1 mm more than those listed in the table.

Table 2.1 Machining allowance for various metals

Material	Shrinkage allowance	Machining allowance for dimensions	
		0–30 cm	30–60 cm
Cast iron	1/96	2.5 mm	4.0 mm
Cast steel (low carbon)	1/48	3 mm	4.5 mm
Aluminium	3/192	1.5 mm	3 mm
Bronze	3/192	1.5 mm	3 mm
Brass	1/48	1.5 mm	3 mm

There is another deviation from the original job dimensions and is intentionally provided in the pattern; this is called *draft*. It refers to a taper put on the surface parallel to the direction of withdrawal of the pattern from the mould cavity. A draft facilitates easy withdrawal of the pattern. The average value of the draft is between $\frac{1}{2}°$ and 2°.

2.2.2 TYPES OF PATTERNS

The commonly-used patterns are classified as follows:

(i) *Loose pattern* It is made in one piece, usually from wood, and is used for castings numbering up to 100.

(ii) *Gated pattern* This is simply one or more than one loose pattern with attached gates and runners and provides a channel through which the molten metal can flow from the pouring sprue to the mould cavity. This pattern is frequently set on a *follow board* conforming to the *parting surface* of the mould. The follow board helps in an easy removal of the pattern after the mould has been prepared.

(iii) *Match plate pattern* This pattern is made in two halves mounted on both sides of a *match plate* (of wood or metal) conforming to the contour of the parting surface. The match plate is accurately placed between the cope and the drag flasks by means of locating pins. For small castings, several patterns can be mounted on the same match plate.

(iv) *Cope and drag pattern* Here, the cope and drag halves of a split pattern (Fig. 2.1) are separately mounted on two match plates. Thus, the cope and the drag flasks are made separately and brought together (with accurate relative location) to produce the complete mould.

(v) *Sweep pattern* Normally made of wood, it is used to generate surfaces of revolution in large castings, and to prepare moulds out of a paste-

like material. Here, "sweep" refers to the section that rotates about an edge to yield circular sections.

(vi) *Skeleton pattern* This consists of a simple wooden frame outlining the shape of the casting. It is used to guide the moulder for hand-shaping the mould and for large castings having simple geometrical shapes.

While designing a pattern, the parting line should be chosen so as to have the smallest portion of the pattern in the cope. As the moulding sand has greater strength in compression than in tension, the heavier sections of the pattern should be included in the drag. The possible defects due to loose sand in the mould are more frequent in the cope half. For this reason, the most critical surface should also be included in the drag. Figure 2.1

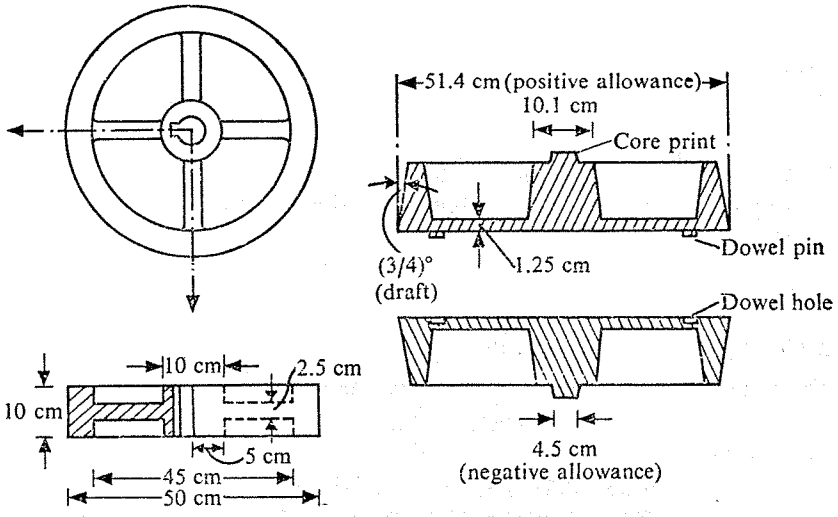

(a) Wheel details (b) Split pattern

Fig. 2.1 Cast iron wheel and its split pattern (shown to a different scale).

shows a typical split pattern (with allowances) for a cast iron wheel. The reader is advised to carefully note all the allowances, positive and negative.

2.2.3 TYPES OF MOULDS

Moulds can be classified on the basis of either the material, i.e., green sand mould, plastic mould, metal mould, or on the method of making them, e.g., shell mould and investment mould. Metal moulds are permanent in the sense that a large number of castings can be made from a single mould; on the other hand, moulds of refractory materials can be used only once. Generally, the green sand moulds are used; in what follows, we shall consider some of their important characteristics. (For a discussion on the other types of moulds, see Section 2.7.)

2.2.4 GREEN SAND MOULD

The material for a green sand mould is a mixture of sand, clay, water, and some organic additives, e.g., wood flour, dextrin, and sea coal. The percentage of these ingredients on weight basis is approximately 70–85% sand, 10–20% clay, 3–6% water, and 1–6% additives. This ratio may vary slightly depending on whether the casting is ferrous or nonferrous.

Sand is an inexpensive refractory material, but natural sand may not have all the desirable qualities of a moulding material. For example, it normally has higher clay content than desired. The sand used as a moulding material should have a specified clay, water, and additive content; in addition, it must have a specific grain size distribution. The importance of the grain size distribution would be clear from the discussion that follows.

Both the shape and the size of sand grains vary over a wide range. The grains may be smooth and round in shape or may have sharp angular corners. The bulk density of a sand-mix is very low if the grains are of almost equal size with smooth round shape. Such grains result in an increased void and a higher permeability. Higher permeability permits an easy outflow of the gases (produced during the casting operation) which may otherwise be entrapped within the casting. The situation gets reversed if the grains are of various sizes and have sharp corners. To study the grain size distribution, the screening test is performed. This is done by taking a fixed sample weight of sand and screening it through standard sieves. The screening is accomplished by shaking the sieves. The amount of sand that collects in the different sieves is then plotted. Finally, from this plot, the distribution of grain size and the average grain size are computed.

Clay, together with water, acts as a bonding agent and imparts tensile and shear strength to the moulding sand. The organic additives burn out at high temperatures and make room for the moulding sand to expand, and thus save the mould from crumbling.

The success of a casting process depends greatly on the properties of the moulding sand. These include (i) strength, (ii) permeability, (iii) deformation, (iv) flowability, and (v) refractoriness. (Standard specimens and tests are recommended for an evaluation of these properties[1].) Strength refers to the compressive strength and deformation indicates the change in length of a standard specimen at the point of failure. Permeability is expressed as the gas flow rate through the specimen under a specified pressure difference across it. Flowability refers to the ability of the sand to flow around and over the pattern when the mould is rammed. Refractoriness measures the ability of the sand to remain solid as a function of temperature. For a given sand-clay ratio, the nature of variation of these properties with water content is as shown in Fig. 2.2. It is obvious, both from strength and permeability considerations, that there is an optimum water content. At a low water content, dry clay powder, being finer than

[1]Datsko, J., Material Properties and Manufacturing Processes, Wiley, New York, 1966

sand grains, fills up the void between the sand particles, and thus reduces

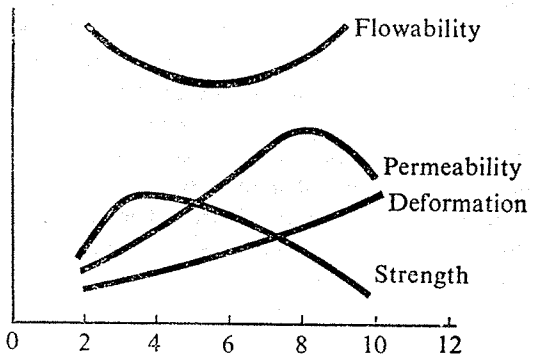

Fig. 2.2 Effect of water content on moulding sand properties.

the permeability. With higher water content, moist clay forms a coating over the sand particles keeping them further away, thus enhancing the permeability. Beyond the optimum water content, water itself fills up the void and reduces the permeability.

2.2.5 PREPARATION OF MOULD

Moulds are made by hand if the number of moulds to be prepared is small. If a large number of simple moulds are required, moulding machines are then used. In this section, we shall briefly discuss some important features of mould making; also, some typical moulding machines will be outlined.

To facilitate an easy removal of the pattern, a parting compound, e.g., nonwetting talc, is dusted on the pattern. Fine grain facing sand is used to obtain a good surface on the casting. Normally, a dead weight is placed on the cope flask to prevent the cope flask from floating due to hydrodynamic forces of the liquid metal. For a large mould, care should be taken to prevent the sand from falling off the cope flask when it is lifted to remove the pattern. This can be done by providing extra supports, called *gaggers*, within the cope flask. For a casting with re-entrant surfaces, e.g., a wheel with a groove at the rim, the mould can be made in three parts (Fig. 2.3). The part between the cope and the drag is termed as the *cheek*. For an easy escape of the gases, vent holes are provided in the cope flask.

The moulding machines operate on one or a combination of the principles explained in Fig. 2.4. In jolt ramming, the mould is lifted through a height of about 5 cm and dropped 50–100 times at a rate of 200 times per minute. This causes somewhat uneven ramming, but is quite suitable for horizontal surfaces. On the other hand, squeezing is found satisfactory for shallow flasks. The sand slinging operation is also very fast and results in

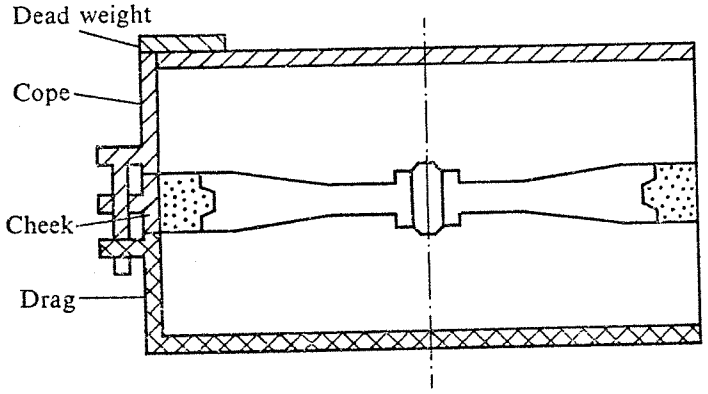

Fig. 2.3 Three-part mould.

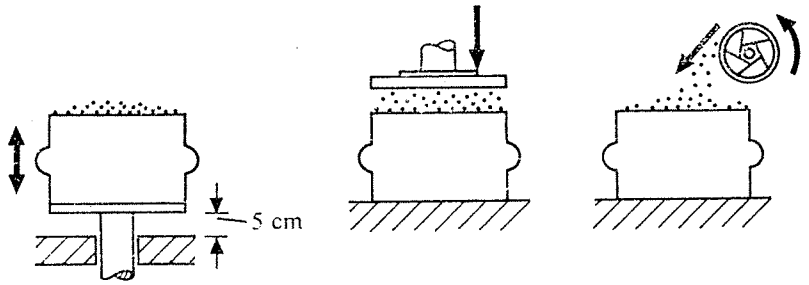

(a) Jolt ramming (b) Squeezing (c) Sand slinging

Fig. 2.4 Principles of machine moulding operation.

uniform ramming. This, however, incurs high initial cost.

2.3 MELTING

A proper care during melting is essential for a good, defect-free casting. The factors to be considered during melting include gases in metals, selection and control of scrap, flux, furnace, and temperature. We shall now give a short discussion on these.

2.3.1 GASES IN METALS

The gases in metals normally lead to faulty castings. However, the presence of a controlled amount of specific gases can be beneficial in imparting certain desirable qualities to the castings. In metal castings, the gases

(i) may be mechanically trapped (in such situations, proper venting arrangements in the mould prevent their occurrence),

(ii) may be generated due to the variation in their solubility at different temperatures and phases, and

(iii) may be produced due to chemical reactions.

The gases most commonly present are hydrogen and nitrogen. Metals are divided into two groups so far as the solubility of hydrogen is concerned. One group is called endothermic; this includes common metals such as aluminium, magnesium, copper, iron, and nickel. The other group, called exothermic, includes, amongst others, titanium and zirconium. Endothermic metals absorb less hydrogen than exothermic metals. Further, in endothermic metals, the solubility of hydrogen increases with temperature. The reverse is true for exothermic metals. In both cases, the solubility (S) can be expressed as

$$S = C \exp [-E_s/(k\theta)], \tag{2.1}$$

where E_s (positive for endothermic) is the heat of solution of 1 mol of hydrogen and θ is the absolute temperature with C and k as constants. Equation (2.1) clearly shows that gas precipitation during cooling cannot take place in exothermic metals for which E_s is negative.

Hydrogen is believed to dissolve interstitially in exothermic metals, thus causing lattice distortion. In endothermic metals, hydrogen dissolves in lattice defects and produces no distortion. Table 2.2 shows the solubility of hydrogen in the solid and liquid phases at solidus temperature for various metals. The difference in these solubilities is responsible for the evolution of the gases. It should be noted that hydrogen solubility is an acute problem

Table 2.2 Solubility of hydrogen in various metals

Pressure = 1 atm		
Metal	Liquid solubility (cc/kg)	Solid solubility (cc/kg)
Iron	270	70
Magnesium	260	180
Copper	55	20
Aluminium	7	0.4

in ferrous casting. Here, although the amount of hydrogen by weight appears negligible, the volume evolved during solidification is quite large. Sievert's law states that the amount of hydrogen dissolved in a melt varies as

$$\% \text{ hydrogen present} = K\sqrt{p_{H_2}}, \tag{2.2}$$

where p_{H_2} is the partial pressure of hydrogen in the atmosphere over the melt, and the constant K can be evaluated from Table 2.2.

The primary sources of hydrogen in a melt are furnace dampness, air, oil, and grease. There is no simple dehydrogenating addition to eliminate hydrogen in the form of slag. So, care should be taken to maintain the hydrogen level to a minimum.

Most hydrogen removal techniques are based on equation (2.2), i.e., reducing the partial pressure of hydrogen by bubbling some other dry insoluble gas through the melt. For nonferrous metals, chlorine, nitrogen, helium, or argon is used. Nitrogen cannot be used for ferrous and nickel based alloys since it is soluble in these, and also it may form nitrides which affect the grain size; therefore, in ferrous alloys in particular, an accurate control of the nitrogen is necessary. In such situations, carbon monoxide bubbles are used. This removes not only hydrogen but also nitrogen; the carbon content is controlled by subsequent oxidation and recarburization. For ferrous metals, a marked decrease in the solubility of nitrogen during the change of phase may give rise to porosity in the casting. The re-entry of nitrogen from the air is prevented by the impermeable slag at the top of the melt.

Currently, vacuum melting is increasingly being used for preventing the solution of gases in metals and the combination of reactive elements in the melt. Additions in the ladle, rather than in the melt, have been found to be more effective for controlling the gases and chemical compositions.

2.3.2 FURNACES

The furnaces used for melting metals differ widely from one another. The selection of a furnace depends mainly on the metal chemistry, the maximum temperature required, and the metal delivery rate and mode. The other important factors in making a selection are the size and shape of the available raw materials.

The metal chemistry decides not only the control of standard elements but also some important mechanical properties, e.g., machinability.

The optimum temperature after melting is decided by a property, called *fluidity*, of the metal. Fluidity refers to the relative ability of the liquid metal to fill in the mould at a given temperature. Normally, the lower the viscosity, the higher the fluidity. The fluidity of a metal can be checked as follows. A spiral of standard dimensions is poured with the liquid metal at various temperatures. The length of the spiral which can be fed in this way before the solidification starts gives the measure of fluidity. If we examine the temperature-fluidity curves for various metals, we find that the higher the fluidity of a metal, the lower the difference needed between the pouring temperature (furnace temperature) and the melting temperature. For completely filling up the intricate, thin sections of the mould, this difference should be a minimum. A large difference implies higher cost and more gas solubility.

The rate and mode of liquid metal delivery are largely decided by the process—batch or continuous melting—used.

Figure 2.5 gives the sketches of various furnaces normally used in foundries; the maximum obtainable temperatures are also shown.

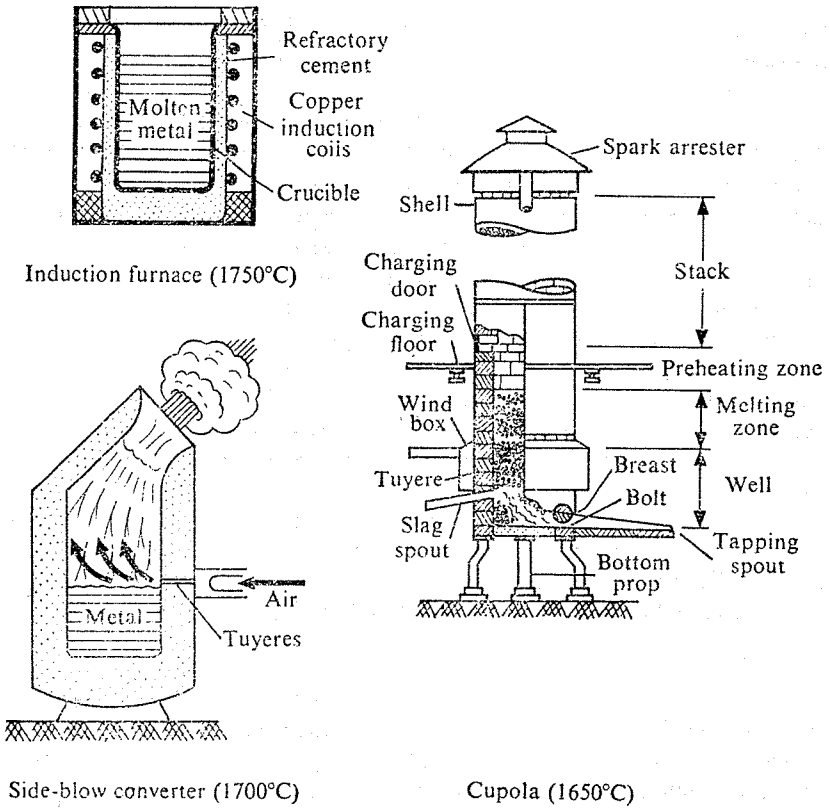

Fig. 2.5 Principal melting furnaces.

2.4 POURING (GATING DESIGN)

After melting, the metal is poured or injected into the mould cavity. We shall now discuss the difficulties faced in doing this and explain how these can be overcome by using an appropriate gating design. A good gating design ensures distribution of the metal in the mould cavity at a proper rate without excessive temperature loss, turbulence, and entrapping gases and slags.

If the liquid metal is poured very slowly, then the time taken to fill up the mould is rather long and the solidification may start even before the mould has been completely filled up. This can be avoided by using too much superheat, but then gas solubility may cause a problem. On the other hand, if the liquid metal impinges on the mould cavity with too high a velocity, the mould surface may be eroded. Thus, a compromise has to be made in arriving at an optimum velocity.

The design of a gating system depends on both the metal and mould compositions. For example, an elaborate gating design is needed to avoid dross (e.g., oxides) in easily oxidized metals of low melting point such as aluminium. For cast iron, however, a short path for the liquid metal is selected to avoid a high pouring temperature. The gating design for a ceramic mould is quite different from that normally used for a permeable sand mould.

Broadly, gating designs can be classified into three categories, namely, (i) vertical gating, (ii) bottom gating, and (iii) horizontal gating. In vertical gating, the liquid metal is poured vertically to fill the mould with atmospheric pressure at the base. In bottom gating, on the other hand, the liquid metal is filled in the mould from bottom to top, thus avoiding the splashing and oxidation associated with vertical gating. Figure 2.6 shows a simple vertical gating and a bottom gating design. In the horizontal gating system, additional horizontal portions are introduced for better distribution of the liquid metal with minimum turbulence.

Simple calculations based on principles of fluid flow can lead to an estimate of the time taken to fill up a mould. We shall illustrate this for the two designs in Fig. 2.6. The integrated energy balance equation on the

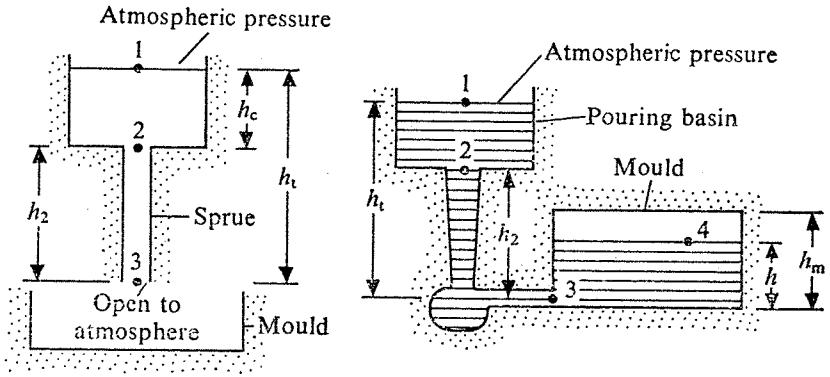

(a) Simple vertical gating (b) Bottom gating

Fig. 2.6 Types of gatings.

basis of per unit mass flow, more commonly known as Bernoulli's equation, will be used. For example, in Fig. 2.6a, it is assumed that the pressure at points 1 and 3 is equal (i.e., $p_1 = p_3$) and that level 1 is maintained constant. Thus, the velocity at station 1 (v_1) is zero. Moreover, the frictional losses are neglected. Then, the energy balance equation between points 1 and 3 gives

$$gh_t = v_3^2/2$$

or

$$v_3 = \sqrt{2gh_t}, \tag{2.3}$$

where g is the acceleration due to gravity and v_3 is the velocity of the liquid

metal at the gate, subsequently referred to as v_g. So, the time taken to fill up the mould (t_f) is obtained as

$$t_f = \frac{V}{A_g v_3}, \tag{2.4}$$

where A_g and V are the cross-sectional area of the gate and the volume of the mould, respectively.

In Fig. 2.6b, applying Bernoulli's equation between points 1 and 3, we get

$$gh_t = \frac{p_3}{\rho_m} + \frac{v_3^2}{2}, \tag{2.5}$$

where ρ_m is the density of the liquid metal, p_3 is the gauge pressure at station 3, and h_t is again assumed to be constant. Further, applying Bernoulli's equation between points 3 and 4, with the assumptions that v_4 is very small and all the kinetic energy at station 3 is lost after the liquid metal enters the mould, we can write

$$p_3/\rho_m = gh. \tag{2.6}$$

From equations (2.5) and (2.6), the velocity of the liquid metal at the gate we obtain is

$$v_g = v_3 = \sqrt{2g(h_t - h)}. \tag{2.7}$$

Equation (2.7) gives the velocity of a jet discharging against a static head h, making the effective head as $(h_t - h)$. Now, for the instant shown, let the metal level in the mould move up through a height dh in a time interval dt; A_m and A_g are the cross-sectional areas of the mould and the gate, respectively. Then,

$$A_m\, dh = A_g v_g\, dt. \tag{2.8}$$

Using equations (2.7) and (2.8), we get

$$\frac{1}{\sqrt{2g}} \frac{dh}{\sqrt{h_t - h}} = \frac{A_g}{A_m}\, dt. \tag{2.9}$$

At $t = 0$, $h = 0$ and at $t = t_f$ (filling time), $h = h_m$. Integrating equation (2.9) between these limits, we have

$$\frac{1}{\sqrt{2g}} \int_0^{h_m} \frac{dh}{\sqrt{h_t - h}} = \frac{A_g}{A_m} \int_0^{t_f} dt$$

or

$$t_f = \frac{A_m}{A_g} \frac{1}{\sqrt{2g}} 2(\sqrt{h_t} - \sqrt{h_t - h_m}). \tag{2.10}$$

If a riser (reservoir to take care of the shrinkage from the pouring temperature) is used, then the pouring time t_f should also include the time needed to fill up the riser. Normally, open risers are filled up to the level of the pouring sprue; thus, the time taken to fill up the riser is calculated with A_m replaced by A_r (riser cross-section) and h_m by h_t in equation (2.10).

EXAMPLE 2.1 Two gating designs for a mould of 50 cm × 25 cm × 15 cm are shown in Fig. 2.7. The cross-sectional area of the gate is 5 cm². Determine the filling time for both the designs.

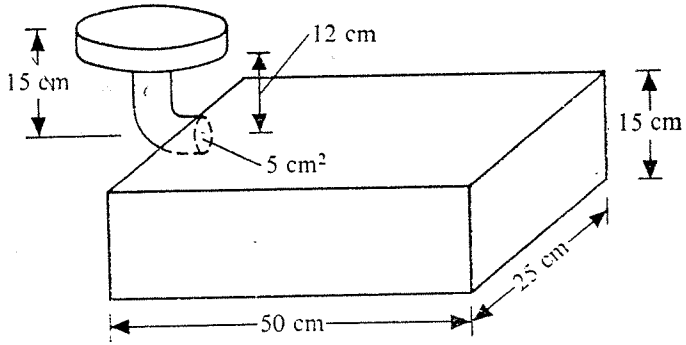

(a) Top gating

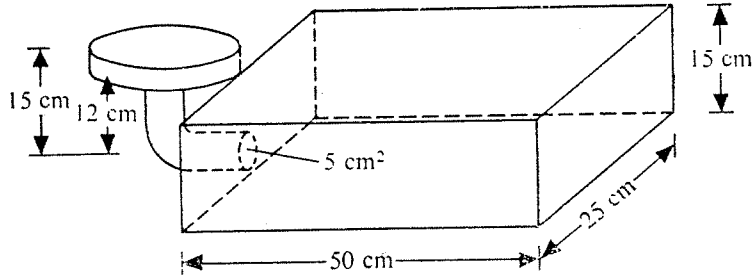

(b) Bottom gating

Fig. 2.7 Top and bottom gating designs.

SOLUTION Figure 2.7a. Since $h_t = 15$ cm, from equation (2.3), we have

$$v_3 = \sqrt{2 \times 981 \times 15}\ \text{cm/sec} = 171.6\ \text{cm/sec}.$$

The volume of the mould is $V = 50 \times 25 \times 15$ cm³ and the cross-sectional area of the gate is $A_g = 5$ cm². So, from equation (2.4), we get

$$t_f = \frac{50 \times 25 \times 15}{5 \times 171.6}\ \text{sec} = 21.86\ \text{sec}.$$

Figure 2.7b. Here, $h_t = 15$ cm, $h_m = 15$ cm, $A_m = 50 \times 25$ cm^2, and $A_g = 5$ cm^2. Using equation (2.10), we have

$$t_f = \frac{50 \times 25}{5} \frac{\sqrt{2}}{\sqrt{981}} \sqrt{15} \text{ sec} = 43.71 \text{ sec}.$$

It should be noted that in Fig. 2.7b the time taken is double of that in Fig. 2.7a. We can easily verify that this will always be so if $h_m = h_t$.

2.4.1 ASPIRATION EFFECT

For a mould made of a permeable material (e.g., sand), care should be taken to ensure that the pressure anywhere in the liquid metal stream does not fall below the atmospheric pressure. Otherwise, the gases originating from baking of the organic compounds in the mould will enter the molten metal stream, producing porous castings. This is known as the aspiration effect.

Referring to Fig. 2.6a and applying Bernoulli's equation between points 2 and 3, we obtain

$$gh_2 + \frac{p_2}{\rho_m} + \frac{v_2^2}{2} = \frac{p_3}{\rho_m} + \frac{v_3^2}{2}, \tag{2.11}$$

where p and v refer to the pressure and velocity, respectively, of the liquid metal at stations 2 and 3. If the pressure at point 3 is atmospheric, i.e., $p_3 = 0$, then $p_2 = -\rho_m g h_2$ as $v_2 = v_3$. Hence, the design in Fig. 2.6a is not acceptable. To avoid negative pressure at point 2 (to ensure positive pressure anywhere in the liquid column), the sprue should be tapered, the ideal shape of which can be determined as follows.

Let, in the limiting case, p_2 be equal to zero, when, from equation (2.11),

$$\frac{v_3^2}{2} = gh_2 + \frac{v_2^2}{2}. \tag{2.12}$$

From the principle of continuity of flow, $A_2 v_2 = A_3 v_3$, where A is the cross-sectional area. Thus,

$$v_2 = \frac{A_3}{A_2} v_3 = R v_3, \tag{2.13}$$

where $R = A_3/A_2$. Using equations (2.12) and (2.13), we obtain

$$\frac{v_3^2}{2g} = h_2 + \frac{R^2 v_3^2}{2g}$$

or

$$R^2 = 1 - \frac{2gh_2}{v_3^2}. \tag{2.14}$$

Again, $v_3^2 = 2gh_t$ (applying Bernoulli's equation between points 1 and 3, with $p_1 = p_3 = 0$ and $v_1 = 0$). Substituting this in equation (2.14), we have

$$R^2 = 1 - \frac{h_2}{h_t} = \frac{h_c}{h_t}$$

or

$$R = \frac{A_3}{A_2} = \sqrt{\frac{h_c}{h_t}}. \tag{2.15}$$

[This can easily be seen to be the shape of a freely falling stream when $v_2 = \sqrt{2gh_c}$ and $v_3 = \sqrt{2gh_t}$.] Thus, ideally, the sprue profile should be as shown by the solid lines in Fig. 2.8 when the pressure throughout the stream is just atmospheric. However, a straight tapered sprue (shown by

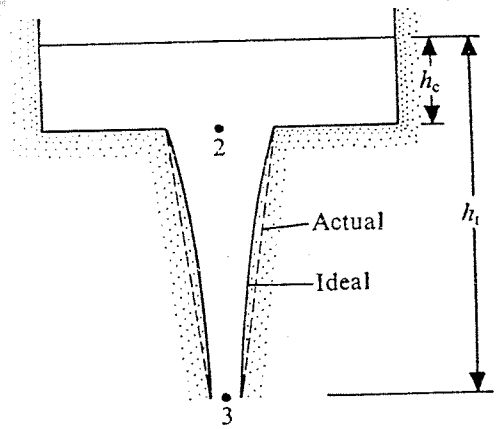

Fig. 2.8 Ideal and actual shapes of sprue.

the dashed lines) is safer (pressure everywhere, except at points 2 and 3, is above atmospheric) and easier to construct. The sprue design in Fig. 2.6b is better than that in Fig. 2.6a.

Another situation where aspiration effect comes into the picture is associated with a sudden change in the flow direction. As shown in Fig. 2.9a, the liquid metal stream contracts around a sharp corner due to the momentum effect. In vertical gating, this has got nothing to do with acceleration due to gravity. The constricted region shown at station 2 in Fig. 2.9a is known as *vena contracta*. To avoid the creation of vacuum around station 2, the mould is made to fit the vena contracta, as done in Fig. 2.9b. In other words, a sharp change in the flow direction is avoided. If the runner diameter is d and the diameter at the entrance is d', then, normally, d'/d is maintained at a value approximately equal to 1.3[1]. This means $r \simeq 0.15d$.

The common items employed in a gating design to prevent impurities in the casting are as follows (see also Fig. 2.10).

[1]Flinn, R.A., Fundamentals of Metal Casting, Addison-Wesley, Reading, Massachusetts, 1963.

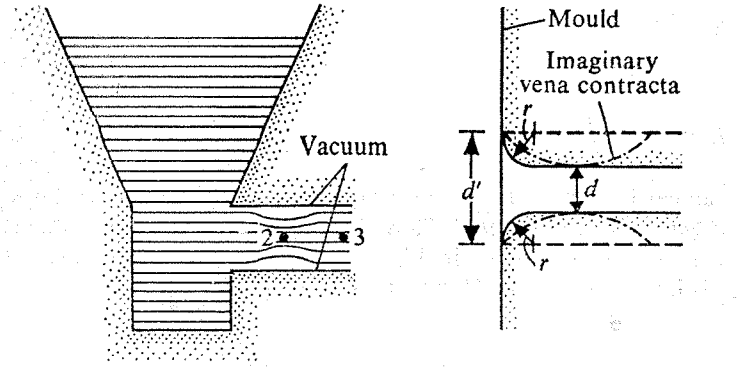

(a) Mechanism of vacuum generation

(b) Outlet dimensions to prevent vacuum generation

Fig. 2.9 Principle of avoiding vacuum generation.

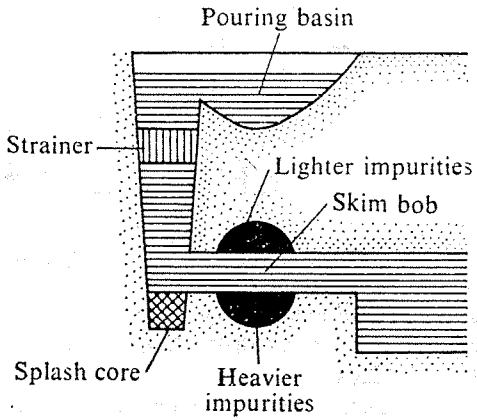

Fig. 2.10 Gating design to prevent impurities.

(i) *Pouring basin* This reduces the eroding force of the liquid metal stream coming directly from the furnace. A constant pouring head can also be maintained by using a pouring basin.

(ii) *Strainer* A ceramic strainer in the sprue removes dross.

(iii) *Splash core* A ceramic splash core placed at the end of the sprue also reduces the eroding force of the liquid metal stream.

(iv) *Skim bob* It is a trap placed in a horizontal gate to prevent heavier and lighter impurities from entering the mould.

2.4.2 EFFECTS OF FRICTION AND VELOCITY DISTRIBUTION

In Sections 2.4 and 2.4.1, we assumed that the velocity of a liquid metal in the sprue and the gate is uniform across the cross-section. In fact, the velocity of a fluid in contact with any solid surface is zero and is maximum at the axis of the conduit. The velocity distribution within the conduit depends on the shape of the conduit and the nature of the flow (i.e., turbulent or laminar). Further, in our discussion so far, we have also assumed no frictional losses. In real fluids, the frictional losses are always present, especially when there is a sudden contraction in or an enlargement of the flow cross-sections. In the discussion that follows, we shall, in the light of these two factors, i.e., velocity distribution and friction, modify the equations we have already developed.

The nonuniform velocity distribution can be accounted for by modifying the kinetic energy term in the integrated energy balance equation by replacing the (velocity)^2 term by $\bar{v}^2/\beta$, where $\bar{v}$ is the average velocity and β is a constant. For a circular conduit, the value of β is equal to 0.5 for laminar flow and approximately equal to 1 for turbulent flow.

The energy loss due to friction in a circular conduit (on the basis of per unit mass) is given by

$$E_{f_1} = 4f\frac{L}{D}\frac{\bar{v}^2}{2}, \tag{2.16}$$

where

$\bar{v}$ = average velocity,

D, L = diameter and length, respectively of the conduit, and

f = friction factor.

The value of f depends on the roughness of the conduit and the nature of the flow. Thus, while using the integrated energy equation between two points, say, 1 and 2, in that order in the direction of flow, E_{f_1} should be added to the energy of station 2.

For a smooth conduit, the value of f is given by the equations

$$f = 16/Re \quad \text{for laminar flow} \qquad (Re < 2000), \tag{2.17}$$

$$\frac{1}{\sqrt{f}} = 4\log_{10}(Re\sqrt{f}) - 0.4 \quad \text{for turbulent flow} \qquad (Re > 2000), \tag{2.18}$$

where Re is Reynolds number. For the range $2100 < Re < 10^5$, equation (2.18) can be simplified to the form

$$f = 0.0791(Re)^{-1/4}. \tag{2.19}$$

Frictional losses also occur due to a gradual change in the flow direction, e.g., in a 90° bend and similar other fittings. In such a situation, the associated frictional losses are accounted for by using equation (2.16) with an equivalent (L/D) factor for the bend.

The frictional loss (per unit mass) associated with a sudden enlargement

or contraction of a flow area is expressed as

$$E_{f_2} = \tfrac{1}{2} e_f \bar{v}^2, \tag{2.20}$$

where $\bar{v}$ is the average velocity of the fluid in the smaller cross-section, and e_f is the friction loss factor and it depends on the ratio of the flow area and Reynolds number of the flow. For a laminar flow, the length and diameter of the smaller flow cross-section have also to be taken into account. The value of e_f depends on whether the flow area is enlarging or contracting in the direction of flow. The values of e_f for a sharp change in the flow cross-section are shown in Figs. 2.11a and 2.11b for sudden expansion and contraction, respectively. In these figures, the Reynolds numbers of the flow have been calculated on the basis of the average flow velocity in the smaller cross-sections, and l and d are the length and diameter, respectively, of the smaller flow cross-sections. The values of e_f for some other types of changes in flow geometry are listed in Fig. 2.12; here, e_{f_s} refers to the values corresponding to a sharp change of geometry with identical initial and final dimensions (i.e., the values of e_{f_s} can be obtained from Figs. 2.11a and 2.11b). Now, going back to Fig. 2.6a, let us modify the analysis presented in Section 2.4 in the light of the effects of friction and velocity distribution.

Using the integrated energy balance equation between points 1 and 3, after accounting for the loss due to a sudden contraction at 2, we get

$$\frac{p_1}{\rho_m} + 0 + g h_t = \frac{p_3}{\rho_m} + \frac{\bar{v}_3^2}{2\beta} + E_{f_1} + E_{f_2}, \tag{2.21}$$

where $\bar{v}_3$ is the average fluid velocity in the sprue. With $p_1 = p_3$ and using equations (2.16) and (2.20), we get

$$2g h_t = \bar{v}_3^2 \left(\frac{1}{\beta} + e_f + 4f\frac{l}{d}\right), \tag{2.22}$$

where d is the diameter of the sprue and l is the length of the sprue ($=h_2$ in Fig. 2.6a). Thus, equation (2.3) can be modified as

$$\bar{v}_3 = C_D \sqrt{2g h_t}, \tag{2.23}$$

where the discharge coefficient

$$C_D = \left(\frac{1}{\beta} + e_f + 4f\frac{l}{d}\right)^{-1/2}. \tag{2.24}$$

In this analysis, we have neglected the fluid velocity (and hence the loss) between points 1 and 2. If the sprue also has a bend or fitting, then E_{f_1} is modified as

$$E_{f_1} = 4f\bar{v}_3^2\left[\frac{l}{d} + \left(\frac{L}{D}\right)_{eq}\right].$$

[The values of $(L/D)_{eq}$ for various types of fittings are listed in standard tables.] In such a case, the discharge coefficient C_D is, finally, given by

$$C_D = \left[\frac{1}{\beta} + e_f + 4f\left\{\frac{l}{d} + \left(\frac{L}{D}\right)_{eq}\right\}\right]^{-1/2}. \tag{2.25}$$

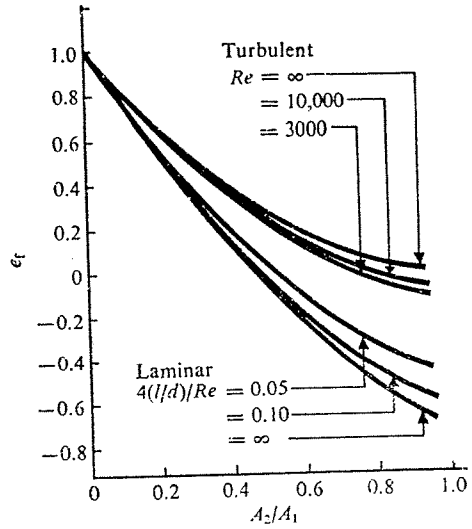

(a) For sudden expansion

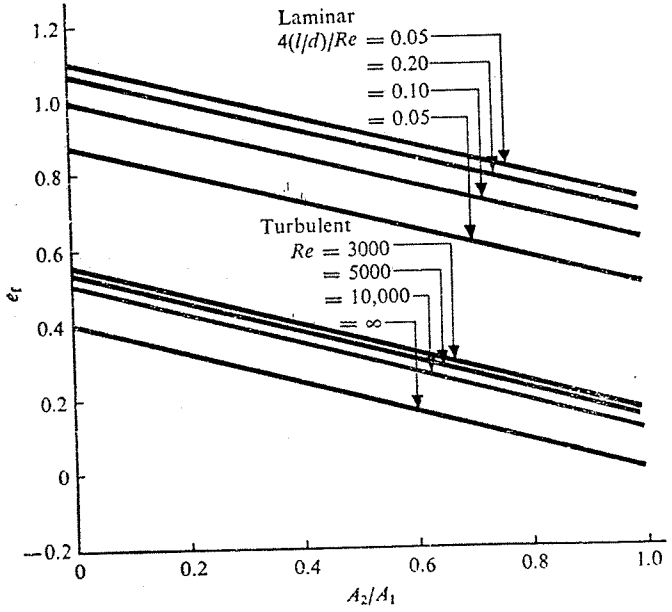

(b) For sudden contraction

Fig. 2.11. Friction loss factor.

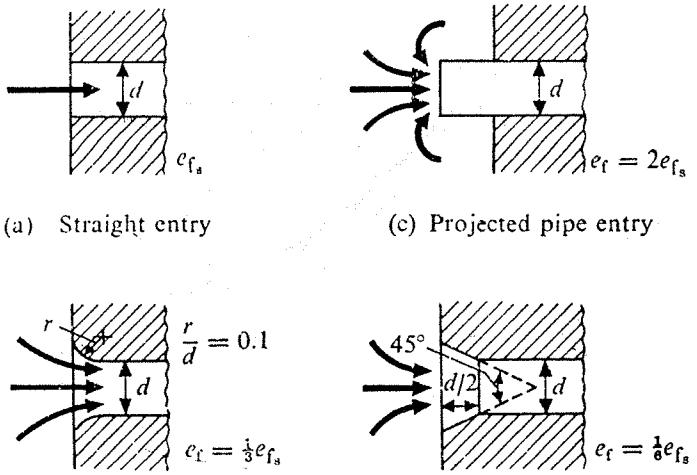

(a) Straight entry (c) Projected pipe entry

(b) Entry with rounded corner (d) Tapered entry

Fig. 2.12 Values of e_f for some types of changes in flow geometry.

EXAMPLE 2.2 Solve Example 2.1 (for Fig. 2.7a) by including the friction and velocity distribution effects. The liquid being poured is molten Fe with the properties $\rho_m = 7800$ kg/m^3, kinetic viscosity $\eta = .00496$ kg/m-sec. For the 90° turn at the end of the sprue, $(L/D)_{eq} = 25$.

SOLUTION It should be noted that to obtain β, f, and e_f (before calculating C_D), we should determine whether the flow is laminar or turbulent. So, the velocity must be determined first. This calls for an iterative procedure as now outlined.

As a first approximation, the average velocity is computed with the assumption that $C_D = 1$. With $C_D = 1$, $\bar{v}_3 = 1.716$ m/sec [see Example 2.1 (for Fig. 2.7a)]. Now, $(\pi/4)\, d^2 = 5$ cm^2 or $d = .0252$ m. Hence, Reynolds number of the flow in the sprue is

$$Re = \frac{\rho_m \bar{v}_3 d}{\eta} = \frac{7800 \times 1.716 \times 0.0252}{0.00496} \approx 68{,}000.$$

So, the flow is turbulent. Thus,

$\beta = 1$,

$e_f \approx 0.45$ [from Fig. 2.11b with $A_2/A_1 \approx 0$, where A_2 and A_1 are the cross-sectional areas of the sprue and the pouring basin, respectively],

$f = \dfrac{0.0791}{(68{,}000)^{1/4}} = 0.0049$ [using equation (2.19)].

Now, using equation (2.25) with $l = 0.12$ m, we have

$$C_D = [1 + 0.45 + 4 \times 0.0049(\frac{0.12}{0.0252} + 25)]^{-1/2} = 0.7.$$

From equation (2.23),

$$\bar{v}_3 = C_D\sqrt{2gh_t} = 0.7 \times 1.716 \text{ m/sec} = 1.20 \text{ m/sec}.$$

We recalculate C_D on the basis of this value of $\bar{v}_3$ until it converges.

For the second approximation,

$$Re = \frac{1.2}{1.716} \times 68{,}000 = 47{,}500$$

when

$\beta = 1$,

$e_f = 0.46$,

$$f = \frac{0.0791}{(47{,}500)^{1/4}} = 0.0054,$$

$$C_D = [1 + 0.46 + 4 \times 0.0054(\frac{0.12}{0.0252} + 25)]^{-1/2}$$

$= 0.69$ (starting value of $C_D = 0.7$).

So

$$\bar{v}_3 = 0.69 \times 1.716 \text{ m/sec} = 1.18 \text{ m/sec}.$$

Thus, the value of $\bar{v}_3$ has converged with sufficient accuracy. Now, using equation (2.4), we find the time taken to fill up the mould is

$$t_f = \frac{V}{A_g \bar{v}_3} = \frac{50 \times 25 \times 15}{5 \times 118} \text{ sec} = 31.7 \text{ sec}.$$

This time is approximately 43% higher than that obtained in Example 2.1 (Fig. 2.7a) (neglecting all the losses).

EXAMPLE 2.3 Figure 2.13 shows a ladle having an internal diameter of 1 m with a capacity height of 1.2 m. It has a 45°-tapered nozzle to a 75-mm exit diameter.

(i) Calculate the time required to empty the ladle if it is filled with an Al-Si alloy at 704°C.

(ii) Estimate the discharge rate in kg/sec (a) initially and (b) when the ladle is 75% empty.

Given

$$\rho_m = 2700 \text{ kg/m}^3, \qquad \eta = 0.00273 \text{ kg/m-sec}.$$

SOLUTION Let at any instant the level of liquid metal be h when the average velocity of the liquid metal through the nozzle is

$$\bar{v}_n = C_D\sqrt{2gh}.$$

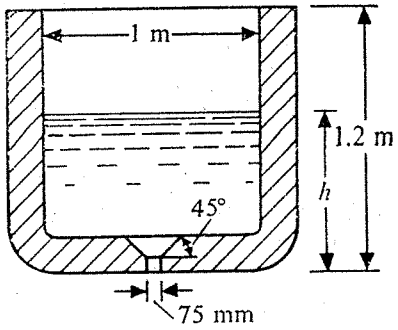

Fig. 2.13 Description of ladle.

The mass flow discharge rate is

$$\dot{m} = \rho_m A_n \bar{v}_n = \rho_m A_n C_D \sqrt{2gh}, \tag{a}$$

where A_n is the nozzle area. Again, $\dot{m} = -\rho_m A_l \, dh/dt$, where A_l is the ladle cross-sectional area. Thus,

$$-\frac{dh}{dt} = \frac{A_n}{A_l} C_D \sqrt{2gh}. \tag{b}$$

This is, of course, under the assumption that C_D remains almost constant for all values of h. Now, the time taken (t_f) for the level to come down from h_i to h_f can be obtained by integrating equation (b) as

$$-\int_{h_i}^{h_f} \frac{dh}{\sqrt{h}} = \frac{A_n}{A} C_D \sqrt{2g} \int_0^{t_f} dt$$

or

$$2(\sqrt{h_i} - \sqrt{h_f}) = \frac{A_n}{A_l} C_D \sqrt{2g} t_f$$

or

$$t_f = \sqrt{\frac{2}{g}} \frac{A_l}{A_n} \cdot \frac{1}{C_D} (\sqrt{h_i} - \sqrt{h_f}). \tag{c}$$

For the given data, let us first examine how C_D varies with h to justify the assumption that C_D remains constant.

First, let us take $h = h_i = 1.2$ m. As a first approximation, we take $C_D = 1$ when

$$\bar{v}_n = \sqrt{2gh} = 4.85 \text{ m/sec},$$

$$Re = \frac{2700 \times 4.85 \times 0.075}{0.00273} = 3.6 \times 10^5.$$

So, the flow is turbulent and consequently

$$\beta = 1,$$

$$e_f = \tfrac{1}{6} e_{f_s} = \tfrac{1}{6} \cdot 0.45 \qquad \text{(from Figs. 2.12 and 2.11b with } A_2/A_1 \approx 0)$$

$$= 0.075.$$

The frictional losses within the ladle are negligible. Hence,

$$C_D = (1 + 0.075)^{-1/2} = 0.96.$$

As this value of C_D is very near unity, there is no need to iterate further (as done in Example 2.2).

Second, let us consider the case when $h \approx 0$, $\bar{v}_n \approx 0$, $Re \to 0$, i.e., the flow is laminar. So, $\beta = \frac{1}{2}$ and $e_f \approx 0.82$. Thus,

$$C_D = (2 + 0.82)^{-1/2} \approx 0.6.$$

Third, let $h = 5$ cm $= 0.05$ m and assume that $C_D = 1$. Then,

$$\bar{v}_n = \sqrt{2 \times 9.81 \times 0.5} \text{ m/sec} \approx 1 \text{ m/sec}.$$

Thus,

$$Re = \frac{2700 \times 1 \times 0.075}{0.00273} = 74175 \qquad \text{(i.e., the flow is turbulent).}$$

So,

$$\beta \approx 1,$$

$$e_f = \tfrac{1}{6} e_{f_s} \approx \tfrac{1}{6} \times 0.45 \approx 0.075 \qquad \text{(again from Figs. 2.12 and 2.11b with } A_2/A_1 \approx 0),$$

i.e.,

$$C_D \approx 0.96.$$

So, C_D remains equal to 0.96 for almost the entire period (except when $h \to 0$), justifying our assumption. We are now in a position to calculate the time and discharge rate.

(i) Here,

$$A_l = \frac{\pi}{4} \times 1 \text{ m}^2 = 0.785 \text{ m}^2,$$

$$A_n = \frac{\pi}{4} \times (0.075)^2 \text{ m}^2 = 4.4 \times 10^{-3} \text{ m}^2 \qquad \text{[with } h_f = 0 \text{ from equation (c)],}$$

$$t_f = \sqrt{\frac{2}{9.81}} \times \frac{0.785}{4.4 \times 10^{-3}} \cdot \frac{1}{0.96} \sqrt{1.2} \text{ sec}$$

$$= 91.9 \text{ sec}.$$

(ii) The initial discharge rate, from equation (a) with $h = 1.2$ m, is given as

$$\dot{m} = 2700 \times 4.4 \times 10^{-3} \times 0.96 \sqrt{2 \times 9.81 \times 1.2} \text{ kg/sec}$$

$$= 55.34 \text{ kg/sec}.$$

The discharge rate when the ladle is 75% empty, i.e., with $h = 0.25 \times 1.2$ m, is obtained from equation (a) as $\dot{m} = 27.67$ kg/sec.

2.5 COOLING AND SOLIDIFICATION

A clear understanding of the mechanism of solidification and cooling of liquid metals and alloys is essential for the production of successful castings. During solidification, many important characteristics such as crystal structure and alloy composition at different parts of the casting are decided. Moreover, unless a proper care is taken, other defects, e.g., shrinkage cavity, cold shut, misrun, and hot tear, also occur.

2.5.1 MECHANISM OF SOLIDIFICATION

Pure Metals

Liquids need to be cooled below their freezing points before the solidification begins. This is because energy is required to create surfaces for new crystals. The degree of supercooling necessary is reduced by the presence of other surfaces (particles) which serve as the initial nuclei for crystal growth. When a liquid metal is poured into a mould, initially (at time t_0 in Fig. 2.14) the temperature everywhere is θ_0. The mould face itself acts

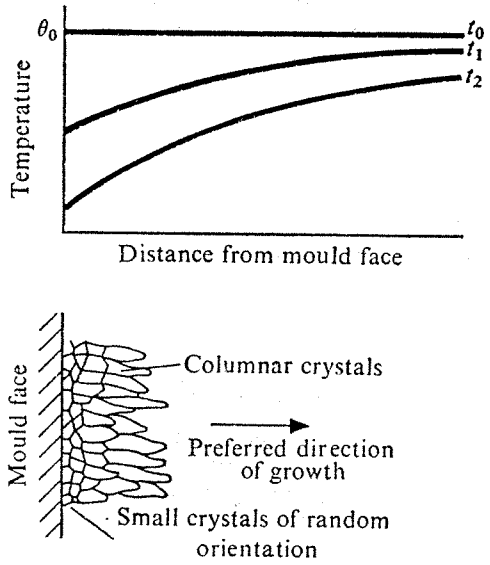

Fig. 2.14 Development of columnar crystals.

as the nucleus for crystal growth, and if the conductivity of the mould is high, randomly-oriented small crystals grow near the mould face. Subsequently, a temperature gradient results within the casting, as indicated in Fig. 2.14 for t_1 and t_2. As the solidification progresses gradually inwards, long columnar crystals, with their axes perpendicular to the mould face, grow. This orientation of crystal growth is desirable from the point of view of strength of the casting.

Alloys

As we have already noted in Chapter 1, an alloy, unlike a pure metal, does not have a sharply defined freezing temperature. The solidification of an alloy takes place over a range of temperature. During this process, the solids separating out at different temperatures possess varying compositions. Due to all these facts, the direction of crystal growth in an alloy depends on various factors, such as

(i) the composition gradient within the casting,

(ii) the variation of solidus temperature with composition, and

(iii) the thermal gradient within the mould.

We shall discuss each of these factors by considering the example of a solid solution alloy whose phase diagram is shown in Fig. 2.15.

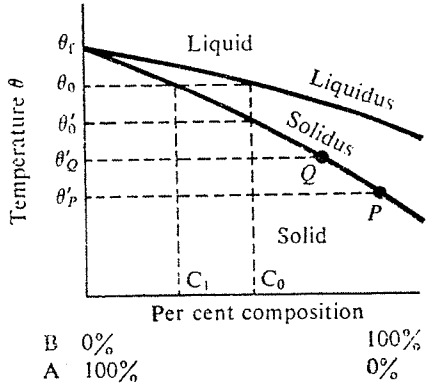

Fig. 2.15 Equilibrium phase diagram of A-B alloy.

Let the liquid alloy have the composition C_0 (of B in A). Also, let θ_f be the freezing point of pure metal A, and θ_0 and θ'_0, respectively, be the liquidus and the solidus temperatures of the alloy of composition C_0. As the liquid alloy is cooled down to the temperature θ_0, solids start to separate out. The concentration of B in these solids is only C_1 ($<C_0$) as is evident from Fig. 2.15. As a result, the concentration of B in the liquid, near the solid-liquid interface, increases to a value more than C_0. Figure 2.16 shows this for the situation where solidification front has progressed up to some distance d from the mould face.

Now, let us consider two points P and Q within the liquid alloy, P being just beyond the solid-liquid interface, as indicated in Fig. 2.16. The solidus temperatures, corresponding to the compositions at P and Q are θ'_P and θ'_Q, respectively (see Fig. 2.15). Let θ_P and θ_Q be the actual temperatures at the points P and Q, respectively. θ_Q is greater than θ_P due to the thermal gradient within the casting (see Fig. 2.14). If both θ_Q and θ_P lie in the range θ'_P to θ'_Q, then the liquid at Q is supercooled, whereas that at P is not. This

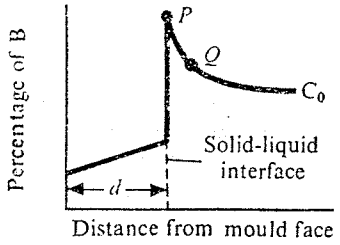

Fig. 2.16 Variation of concentration of B with distance from mould face.

implies that the crystallization starts at Q sooner than at P. If this difference is very prominent, then the columnar growth of crystals starting from the mould surface is hampered. The crystal growth in such a situation may appear as in Fig. 2.17. Thus, a dendritic structure is produced. If the crystal-

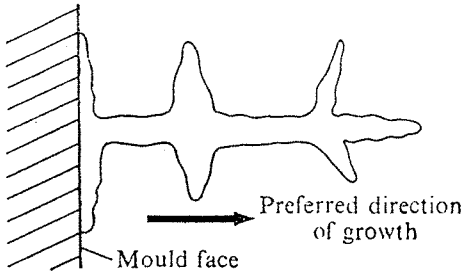

Fig. 2.17 Dendritic crystal growth structure.

lization at Q gets completed before it starts at P (due to a very small thermal gradient, with a very high concentration difference and a very slopy solidus line), then randomly-orientated crystals may appear inside the casting. Moreover, the presence of solid crystals ahead of the solid-liquid interface makes feeding of the liquid metal more difficult. This also implies greater risk of having voids within the casting, normally referred to as *centre-line shrinkage*.

One remedy to avoid the aforestated problem is to produce a large thermal gradient within the mould by providing a *chill* (cooled metal block with high thermal conductivity) at the mould's end. If θ_P is considerably below θ_Q, then the degree of supercooling is not significantly different at P and Q and a gradual progress of the solid-liquid interface is ensured. The problem is obviously less critical for alloys having a small temperature difference between the liquidus and the solidus lines.

The freezing patterns of a chilled and an ordinary mould are shown in Fig. 2.18. In Fig. 2.18a, the solidification starts at the centre line of the

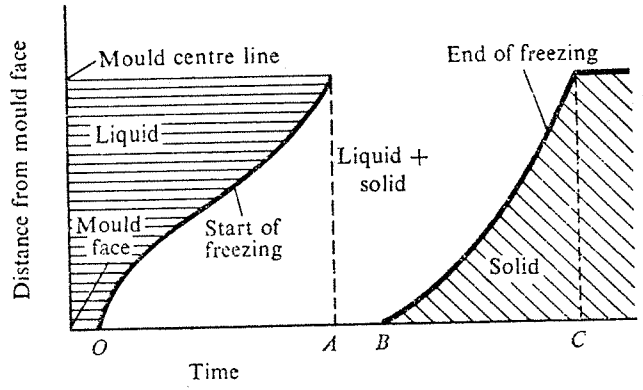

(a) Freezing diagram for ordinary sand mould

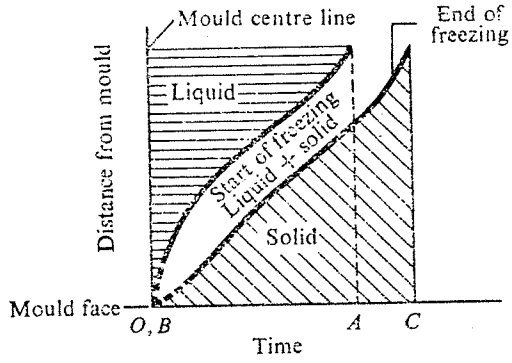

(b) Freezing diagram for chilled mould

Fig. 2.18 Performance of ordinary sand and chilled moulds.

mould before the solidification is complete even at the mould face. In the chilled mould (Fig. 2.18b), on the other hand, due to rapid heat extraction, a narrow liquid-solid zone quickly sweeps across the molten metal.

The difficulty of feeding a given alloy in a mould is expressed by a quantity, called *centre-line feeding resistance* (CFR). It is defined as

$$\text{CFR} = \frac{\text{time interval between start and end of freezing at centre line}}{\text{total solidification time of casting}} \times 100\%.$$

Referring to Fig. 2.18, we find that

$$\text{CFR} = \frac{AC}{OC} \times 100\%. \tag{2.26}$$

Normally, feeding is considered to be difficult if CFR $> 70\%$.

2.5.2 RATE OF SOLIDIFICATION

A reservoir of liquid metal, called riser, is used to compensate for the shrinkage that takes place from the pouring temperature up to solidification (i.e., during the first two phases mentioned in Section 2.2.1). In this respect, grey cast iron is an interesting exception where solidification occurs in two stages. The shrinkage associated with the first stage may well be compensated by the *expansion* that takes place during the second stage, and as such, a riser may not be necessary. To ensure that the riser does not solidify before the casting, we should have an idea of the time taken by the casting to solidify. Moreover, the placement (location) of the riser can be judiciously chosen if an estimate of the time taken by the casting to solidify up to a certain distance from the mould face is available.

The heat rejected by the liquid metal is dissipated through the mould wall. The heat, released as a result of cooling and solidification of the liquid metal, passes through different layers. The temperature distribution in these layers, at any instant, is schematically shown in Fig. 2.19. The thermal

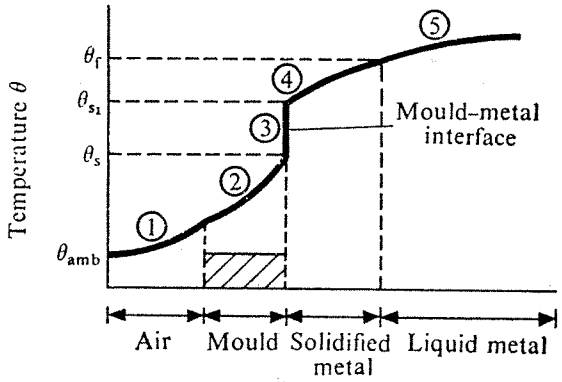

Fig. 2.19 Temperature distribution in different layers.

resistances which govern the entire solidification process are those of the liquid, the solidified metal, the metal-mould interface, the mould, and the ambient air. These five different regions are indicated by the numbers 1 to 5 in Fig. 2.19. The solidification process is quite complicated especially when complex geometry, freezing of alloys, or temperature dependence of thermal properties is considered. In what follows, we shall discuss the solidification of pure metals in some cases of practical interest. In doing so, we shall, depending on the situation, make simplifying assumptions to neglect the thermal resistance of one or more of the regions shown in Fig. 2.19.

2.5.3 SOLIDIFICATION OF A LARGE CASTING IN AN INSULATING MOULD

During the solidification of a large casting in an insulating mould, like the one used in the sand or investment casting (see Section 2.7), almost the entire thermal resistance is offered by the mould. Hence, the analysis we give computes the freezing time by considering only the thermal resistance of region 2 (Fig. 2.19).

Consider a mould face AB shown in Fig. 2.20. The large mould, initially at a temperature θ_0, is assumed to be extended up to infinity in the x-direc-

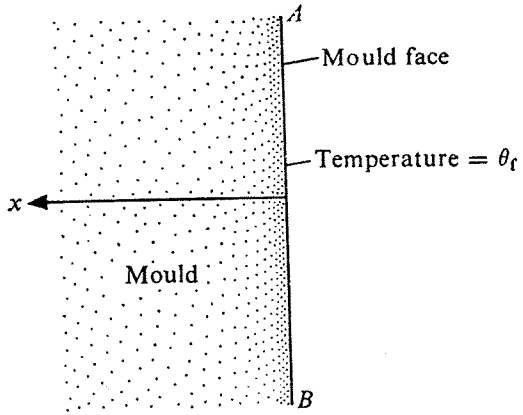

Fig. 2.20 Mould face and coordinate system.

tion. At time $t = 0$, the liquid metal at temperature θ_p is poured into the mould. We also assume that the metal just in contact with the mould face solidifies instantaneously. In other words, the temperature of the mould face is raised to θ_f (freezing temperature of the metal) at $t = 0$ and is maintained at that value till the completion of solidification. The temperature distribution within the mould at a subsequent time t (assuming one-dimensional heat conduction in the x-direction) for such a case is given by[1]

$$\theta_x(t) = \theta_0 + (\theta_f - \theta_0)\left[1 - \operatorname{erf}\frac{x}{2\sqrt{\alpha t}}\right], \tag{2.27}$$

[1]Carslaw, H.S. and Jaeger, J.C., Conduction of Heat in Solids, Clarendon Press, Oxford, 1959.

erf (z) is called the error function. This function is very useful for heat conduction problems in semi-infinite mediums. It represents the convergent series

$$\operatorname{erf}(z) = \frac{2}{\sqrt{\pi}}\left(z - \frac{z^3}{3\cdot 1!} + \frac{z^5}{5\cdot 2!} - \frac{z^7}{7\cdot 3!} + \ldots\right) \tag{2.28}$$

or the integral

$$\operatorname{erf}(z) = \frac{2}{\sqrt{\pi}}\int_0^z e^{-x^2}\,dx. \tag{2.29}$$

The values of this function for various values of its argument z are given in mathematical tables and handbooks. We shall use the result

$$\frac{d}{dz}\operatorname{erf}(z) = \frac{2}{\sqrt{\pi}}e^{-z^2} \tag{2.30}$$

in this chapter.

where $\theta_x(t)$ is the temperature at a distance x from the mould face at an instant t and α is thermal diffusivity of the mould material and is equal to $k/(\rho c)$ with k = conductivity, ρ = density, and c = specific heat of the mould material. Now, the rate of heat flow through the mould face of any instant t is given by

$$\dot{Q} = -kA \frac{\partial \theta_x}{\partial x}\bigg|_{x=0},$$

where A is the cross-sectional area of the mould-metal interface (approximately the surface area of the casting). Using equations (2.27) and (2.30), we obtain

$$\dot{Q} = \frac{kA(\theta_f - \theta_0)}{\sqrt{\pi \alpha t}}. \tag{2.31}$$

Thus, the total quantity of heat flow across the mould face up to a certain time t_0 is

$$Q_{t_0} = \int_0^{t_0} \dot{Q}\, dt = \frac{2Ak(\theta_f - \theta_0)}{\sqrt{\pi \alpha}} \sqrt{t_0}. \tag{2.32}$$

Next, let us calculate the heat the liquid metal rejects in order to solidify. If the liquid metal has a latent heat L, a specific heat c_m, and a density ρ_m, then the heat rejected is given by

$$Q_R = \rho_m V[L + c_m(\theta_p - \theta_f)], \tag{2.33}$$

where V is the total volume of the casting. Hence, the solidification time t_s, obtained by equating (2.32) and (2.33) at t_s, is

$$\frac{2Ak(\theta_f - \theta_0)}{\sqrt{\pi \alpha}} \sqrt{t_s} = \rho_m V[L + c_m(\theta_p - \theta_f)]$$

or

$$t_s = \gamma \left(\frac{V}{A}\right)^2, \tag{2.34}$$

where the constant γ is given by

$$\gamma = \left\{\frac{\rho_m \sqrt{\pi \alpha}[L + c_m(\theta_p - \theta_f)]}{2k(\theta_f - \theta_0)}\right\}^2. \tag{2.35}$$

It should be noted that the foregoing analysis assumes a plane metal-mould interface AB, not usually encountered in engineering practice. Often, we are required to find out the freezing time of complex contours. For such contours, all we need to do is observe (without any precise calculations) the following basic features to know whether the analysis we have given underestimates or overestimates the actual freezing time. To observe these features, we consider three types of metal-mould interfaces (see Fig. 2.21), namely, (i) convex, (ii) plane (used in our analysis), and (iii) concave.

In Fig. 2.21a, the heat flow is more divergent, and consequently the rate is somewhat more than that in Fig. 2.21b. Thus, the freezing time in such a case is overestimated by the foregoing analysis. Similarly, in Fig. 2.21c, the heat flow is more convergent, and consequently the rate is somewhat less than that in Fig. 2.21b. So, the freezing time in such a case is underestimated by the analysis we have given.

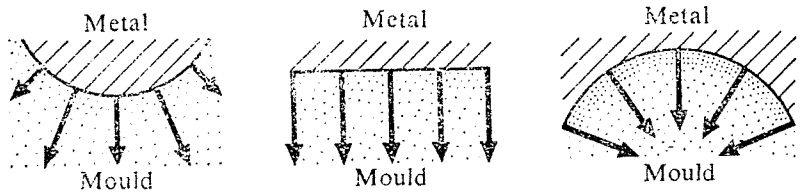

(a) Convex (b) Plane (c) Concave

Fig. 2.21 Heat flow across various types of metal-mould interfaces.

The quantitative results of the effect of the mould-casting interface on the freezing time can be obtained for some basic shapes. Before we give these results, we define two nondimensional parameters, namely,

$$\beta = \frac{V/A}{\sqrt{\alpha t_s}}, \tag{2.36a}$$

$$\lambda = \frac{\theta_f - \theta_0}{\rho_m L'} \rho c \tag{2.36b}$$

with

$$L' = L + c_m(\theta_p - \theta_f). \tag{2.36c}$$

In terms of these parameters, equation (2.34) can be rewritten as

$$\beta = \lambda \frac{2}{\sqrt{\pi}} \quad \text{(for an infinite plane)}. \tag{2.37}$$

A similar result for an infinitely long cylinder is

$$\beta = \lambda \left(\frac{2}{\sqrt{\pi}} + \frac{1}{4\beta}\right) \tag{2.38}$$

and for a sphere is

$$\beta = \lambda \left(\frac{2}{\sqrt{\pi}} + \frac{1}{3\beta}\right). \tag{2.39}$$

EXAMPLE 2.4 A large plate of cross-sectional area A is being cast. Establish a relationship between the time after pouring and the distance of the solidification front from the mould face (Fig. 2.22), assuming no superheat.

SOLUTION During the solidification of this plate-shaped casting, most of the heat is rejected through two side faces, each having the cross-sectional area A. The heat rejected through the other four faces (having very small area as compared with A) is negligible. So, the solidification fronts move from the two sides, as indicated in Fig. 2.22.

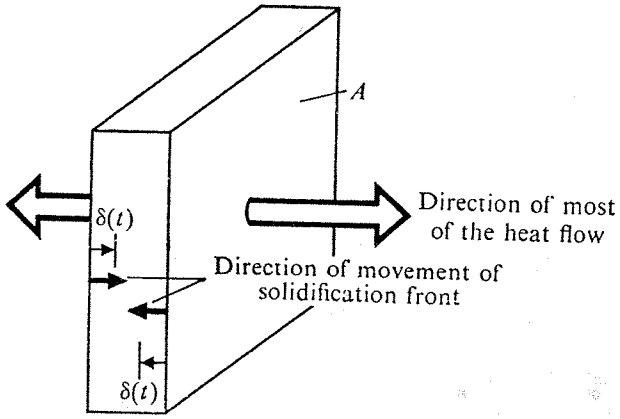

Fig. 2.22 Movement of solidification fronts.

If the solidification fronts move through a distance $\delta(t)$ at any instant t from the respective mould-metal interfaces, then the heat rejected by each solidified half is

$$Q_R = \rho_m A \delta L. \tag{a}$$

Now, the time taken to reject this much of heat through the mould face of the area A is t. Then, from equation (2.32),

$$Q_R = \frac{2Ak(\theta_f - \theta_0)}{\sqrt{\pi\alpha}}\sqrt{t}. \tag{b}$$

Equating the right-hand sides of (a) and (b), we get

$$t = \gamma\delta^2$$

or

$$\delta(t) = \frac{1}{\sqrt{\gamma}}\sqrt{t}, \tag{c}$$

where γ is given by equation (2.35).

A smooth progress of the solidification fronts, as envisaged in the foregoing problem, is not observed in real life, especially in the case of alloys. In fact, all our foregoing analyses should be used only to provide an estimate and not the precise answer.

EXAMPLE 2.5 Determine the solidification time of the following two iron castings when both are poured, with no superheats, into sand moulds at the initial temperature 28°C:

(i) A slab-shaped casting 10 cm thick.

(ii) A sphere 10 cm in diameter.

The data for iron is

$$\theta_f = 1540°C, \qquad L = 272 \text{ kJ/kg}, \qquad \rho_m = 7850 \text{ kg/m}^3;$$

and for sand is

$$c = 1.17 \text{ kJ/kg-K}, \qquad k = 0.8655 \text{ W/m-K}, \qquad \rho = 1600 \text{ kg/m}^3.$$

SOLUTION (i) Let l, b, and h be the length, breadth, and thickness, respectively, of the slab. So, the volume of the casting is

$$V = lbh$$

and the surface area of the casting is

$$A = 2(lb + bh + lh) \approx 2lb \qquad \text{(as both } l, b \gg h\text{)}.$$

Hence,

$$\frac{V}{A} \approx \frac{h}{2} = 5 \times 10^{-2} \text{ m}.$$

As superheat is zero, $\theta_p = \theta_f$, $L' = L$, and $\theta_0 = 28°C$. Using equation (2.36b), we find that

$$\lambda = \frac{(1540 - 28) \times 1600 \times 1.17 \times 10^3}{7850 \times 272 \times 10^3} = 1.3256.$$

So, from equation (2.37),

$$\beta = \frac{2}{\sqrt{\pi}} \times 1.3256 = 1.4957.$$

Now,

$$\alpha = \frac{k}{\rho c} = \frac{0.8655}{1600 \times 1.17 \times 10^3} \text{ m}^2/\text{sec} = 0.46 \times 10^{-6} \text{ m}^2/\text{sec}.$$

Using equation (2.36a), we have

$$\alpha t_s = \frac{(V/A)^2}{\beta^2} = \frac{25 \times 10^{-4}}{2.24} \text{ m}^2.$$

So, the solidification time

$$t_s = \frac{25 \times 10^{-4}}{2.24 \times 0.46 \times 10^{-6}} \text{ sec} = 2430 \text{ sec} = 0.675 \text{ hr}.$$

(ii) Using equation (2.39) with $\lambda = 1.3256$, we obtain

$$\beta = 1.4957 + \frac{0.4419}{\beta} \quad \text{or} \quad \beta^2 - 1.4957\beta - 0.4419 = 0.$$

If we take only the positive real root, then $\beta = 1.75$. Now, for a sphere of radius $R(=5$ cm),

$$\frac{V}{A} = \frac{(4/3)\pi R^3}{4\pi R^2} = \frac{R}{3} = \frac{5}{3} \times 10^{-2} \text{ m}.$$

Again, using equation (2.36a), we find

$$\alpha t_s = \frac{(V/A)^2}{\beta^2} = \frac{25}{9} \times \frac{10^{-4}}{3.05} \text{ m}^2$$

or

$$t_s = \frac{25}{9} \times \frac{10^{-4}}{3.05} \times \frac{10^6}{0.46} \text{ sec} = 198 \text{ sec} = 0.055 \text{ hr}.$$

2.5.4 SOLIDIFICATION WITH PREDOMINANT INTERFACE RESISTANCE

In some common casting processes, the heat flow is controlled significantly by the thermal resistance of the mould-metal interface (indicated as region 3 in Fig. 2.19). These processes include permanent mould casting and die casting. The condition of no contact resistance exists only when the mould-metal contact is so intimate that a perfect wetting occurs, i.e., the casting gets soldered to the mould face. In this section, we shall consider the solidification process assuming that the thermal resistance at the interface is of over-riding importance. In such a case, the temperature distribution, assuming no superheat, is as shown in Fig. 2.23. We are considering again a problem of one-dimensional heat flow. Here, the rate of heat flow

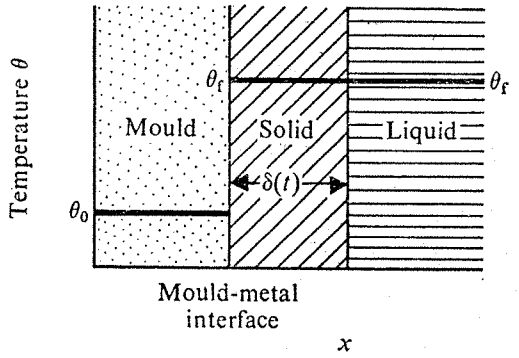

Fig. 2.23 Temperature distribution in mould, and solidified and liquid metal.

through the interface is

$$\dot{Q} = h_f(\theta_i - \theta_0)A, \tag{2.40}$$

where h_f is the film heat transfer coefficient of the interface and A is the surface area of the interface. If the solidification front at this instant is at a distance δ from the mould face, then, on solidification,

$$\text{rate of heat released} = \rho_m A L \frac{d\delta}{dt}. \tag{2.41}$$

Therefore, equating the right-hand sides of (2.40) and (2.41), we have

$$\frac{d\delta}{dt} = \frac{h_f(\theta_f - \theta_0)}{\rho_m L}. \tag{2.42}$$

Integrating this equation with $\delta = 0$ at $t = 0$, we get

$$\delta(t) = \frac{h_f(\theta_i - \theta_0)}{\rho_m L} t. \tag{2.43}$$

Comparing equation (2.43) with equation (c) of Example 2.4, we see that, in the former, the depth of solidification increases linearly with time, whereas in the latter, it is proportional to the square root of time. The total heat rejected by the casting is given by equation (2.33) with $\theta_p = \theta_f$. The heat flow through the interface during the period of solidification t_s is $h_f(\theta_f - \theta_0)At_s$. So, t_s is obtained by equating this expression with equation (2.33), after substituting $\theta_p = \theta_f$, as

$$t_s = \frac{\rho_m L}{h_f(\theta_f - \theta_0)} \cdot \frac{V}{A}. \tag{2.44}$$

Equation (2.44) is helpful in estimating the solidification time of small, thin-section parts cast in a heavy metal mould as used in a die or permanent mould casting.

It may be noted at this stage that over and above the interface resistance we have discussed, there are significant differences between the solidification process in a sand mould and that in a chill or metal mould. We give here two important ways in which the latter differs from the former:

(i) The thermal conductivity of the solidified metal may provide considerable thermal resistance, as shown by region 4 of Fig. 2.19. Because of this, the surface temperature of the casting (θ_s), as can be seen, becomes much lower than the freezing temperature θ_f.

(ii) Because of the subcooled solidified metal, more total heat than that considered in the earlier sections has to be removed. Thus, the heat capacity of the solidifying metal also plays an important role in the rate of solidification.

We shall see more of these two aspects in Sections 2.5.5 and 2.5.6 where additional examples of the solidification process will be considered.

2.5.5 SOLIDIFICATION WITH CONSTANT CASTING SURFACE TEMPERATURE

If a large, slab-shaped casting (say, of steel) is produced in a thin, water cooled mould made out of a metal (say, of copper) having a much higher conductivity than the solidified casting, then the thermal resistance provided by the solidifying metal itself is significant. In such a case, the predominant thermal resistance is offered by region 4 (see Fig. 2.19). Neglecting the thermal resistances of all the other regions, the temperature distribution at any instant takes the shape shown in Fig. 2.24. Here, the mould-metal interface (or the casting surface) temperature θ_s can be assumed to

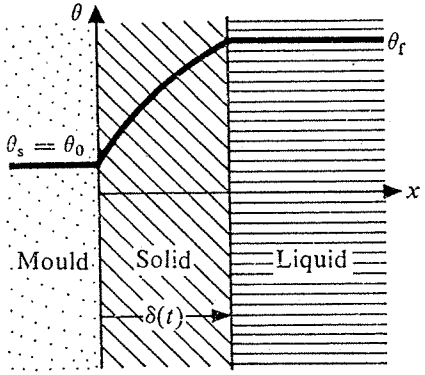

Fig. 2.24 Temperature distribution with constant casting surface temperature.

remain constant at its initial value θ_0, and θ_f indicates the freezing temperature of the metal and this is also taken as the pouring temperature. At any instant t, $\delta(t)$ indicates the depth of solidification. The process can be idealized, without much error, as a one-dimensional one. Hence, the solidification time t_s is obtained from $\delta(t_s) = h/2$, where h is the thickness of the slab being cast. The temperature profile within the range $0 < x < \delta(t)$ is given by[1]

$$\frac{\theta - \theta_s}{\theta_\infty - \theta_s} = \text{erf}\left(\frac{x}{2\sqrt{\alpha_s t}}\right), \tag{2.45}$$

where α_s is the thermal diffusivity of the solidified metal and θ_∞ is a constant of integration. At $x = \delta(t)$, $\theta = \theta_f$; substituting these in equation (2.45), we get

$$\text{erf}\left[\frac{\delta(t)}{2\sqrt{\alpha_s t}}\right] = \frac{\theta_f - \theta_s}{\theta_\infty - \theta_s} = \text{constant} = \lambda\,(\text{say}). \tag{2.46}$$

[1]Geiger, G.H. and Poirier, D.R., Transport Phenomena in Metallurgy, Addison-Wesley, Reading, Massachusetts, 1973.

Hence,

$$\delta(t) = 2\zeta\sqrt{\alpha_s t}, \tag{2.47}$$

where $\text{erf}\,(\zeta) = \lambda$. Once again, we find the depth of solidification varies as the square root of time. Now, the constant ζ can be determined as follows. Considering the rate of energy flow balance at the solid-liquid interface, we have

$$k_s \left.\frac{\partial\theta}{\partial x}\right|_{x=\delta} = \rho_m L \frac{d\delta}{dt}, \tag{2.48}$$

where

k_s = conductivity of the solidified metal = $\alpha_s \rho_m c_s$,

ρ_m = density of the metal (same in the solid and the liquid states),

c_s = specific heat of the solidified metal, and

L = latent heat of fusion of the metal.

From equation (2.45),

$$\frac{\partial\theta}{\partial x} = (\theta_\infty - \theta_s)\frac{d}{dx}\left[\text{erf}\left(\frac{x}{2\sqrt{\alpha_s t}}\right)\right]$$

$$= (\theta_\infty - \theta_s)\frac{1}{2\sqrt{\alpha_s t}}\frac{2}{\sqrt{\pi}}$$

$$\times \exp\left[-\left(\frac{x}{2\sqrt{\alpha_s t}}\right)^2\right] \quad \text{[using equation (2.30)]}. \tag{2.49}$$

Again, using equation (2.49) in equation (2.48), we obtain

$$\frac{k_s}{\sqrt{\alpha_s}}(\theta_\infty - \theta_s)\frac{1}{\sqrt{\pi t}}\exp\left[-\left(\frac{\delta}{2\sqrt{\alpha_s t}}\right)^2\right] = \rho_m L \frac{d\delta}{dt}. \tag{2.50}$$

Now, substituting from equations (2.46) and (2.47) for $(\theta_\infty - \theta_s)$ and δ, respectively, and simplifying, we can rewrite equation (2.50) as

$$\sqrt{k_s \rho_m c_s}\frac{(\theta_f - \theta_s)}{\text{erf}\,(\zeta)}\frac{1}{\sqrt{\pi t}}e^{-\zeta^2} = \rho_m L \zeta \sqrt{\alpha_s}\frac{1}{\sqrt{t}}$$

or

$$\zeta e^{\zeta^2}\,\text{erf}\,(\zeta) = \frac{(\theta_f - \theta_s)}{\sqrt{\pi}}\frac{c_s}{L}. \tag{2.51}$$

The solution of equation (2.51) for ζ can be obtained by trial and error. A simpler procedure is to first plot a graph of $\zeta e^{\zeta^2}\,\text{erf}\,(\zeta)$ for various values of ζ. Then, from this graph, the value of ζ corresponding to the value of the right-hand side of equation (2.51) can be obtained. Thus, once ζ is known, the solidification time t_s can be obtained, from equation (2.47) with

$\delta(t_s) = h/2$, as

$$2\zeta\sqrt{\alpha_s t_s} = \frac{h}{2} \quad \text{or} \quad t_s = \frac{h^2}{16\zeta^2\alpha_s}. \tag{2.52}$$

This analysis is valid only after the initial solidification stage (0.5–1 cm) is over. Similar results for the solidification time of the other shapes can be found from the available literature.

2.5.6 SOLIDIFICATION WITH PREDOMINANT RESISTANCE IN MOULD AND SOLIDIFIED METAL

Let us now consider the problem discussed in Section 2.5.5 under a little different situation. We assume that the copper mould is quite thick and is not water cooled. Then, the mould-metal interface temperature θ_s can no longer be assumed to remain at its initial value θ_0. The value of θ_s, still assumed to be constant, is decided by the thermal properties of the mould and the solidified metal. Moreover, after the initial stage of solidification, the interface resistance also becomes negligible. Thus, the only significant thermal resistance is offered by regions 2 and 4 (Fig. 2.19) and the resulting temperature distribution at any instant is as shown in Fig. 2.25. Assuming

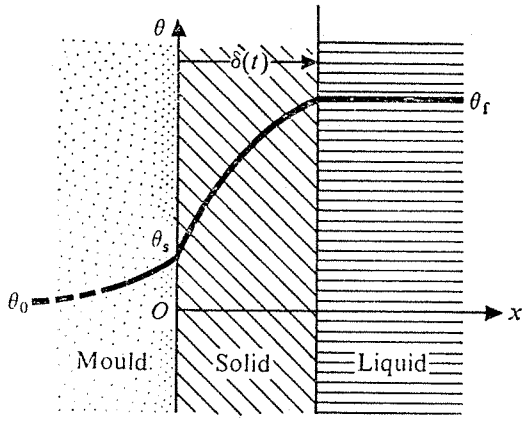

Fig. 2.25 Temperature distribution.

the mould to be a semi-infinite medium in the negative x-direction, the temperature distribution in the mould is[1]

$$\frac{\theta - \theta_s}{\theta_0 - \theta_s} = \text{erf}\left(-\frac{x}{2\sqrt{\alpha t}}\right) \quad \text{for } x < 0 \tag{2.53}$$

and that in the solidified metal is

$$\frac{\theta - \theta_s}{\theta_\infty - \theta_s} = \text{erf}\left(\frac{x}{2\sqrt{\alpha_s t}}\right) \quad \text{for } x > 0, \tag{2.54}$$

[1]Geiger, G.H. and Poirier, D.R., Transport Phenomena in Metallurgy, Addison-Wesley, Reading, Massachusetts, 1973.

where θ_0 is the initial temperature of the mould, θ_s is the mould-metal interface temperature ($\neq\theta_0$), and θ_∞ is a constant of integration. The other conditions to be satisfied are

(i) the balance of heat flux at the mould-metal interface, i.e.,

$$k_s\frac{\partial\theta}{\partial x}\bigg|_{x=0+} = k\frac{\partial\theta}{\partial x}\bigg|_{x=0-}, \tag{2.55}$$

(ii) the rate of energy flow balance at the solid-liquid interface [see equation (2.48)], i.e.,

$$k_s\frac{\partial\theta}{\partial x}\bigg|_{x=\delta} = \rho_m L\frac{d\delta}{dt}, \tag{2.56}$$

(iii)

$$\theta(\delta, t) = \theta_f. \tag{2.57}$$

Equations (2.53)–(2.57) can be combined to give the three equations

$$\frac{(\theta_f - \theta_s)c_s}{L\sqrt{\pi}} = \zeta e^{\zeta^2}\,\text{erf}\,(\zeta), \tag{2.58}$$

$$\frac{(\theta_\infty - \theta_s)c_s}{L\sqrt{\pi}} = \zeta e^{\zeta^2}, \tag{2.59}$$

$$\frac{\theta_s - \theta_0}{\theta_\infty - \theta_s} = \left(\frac{k_s\rho_m c_s}{k\rho c}\right)^{1/2} = \phi\ (\text{constant}), \tag{2.60}$$

where ζ is the same as in Section 2.5.5. The three unknowns, namely, θ_s, θ_∞, and ζ, can be solved from equations (2.58)–(2.60) as follows. Using equations (2.59) and (2.60), we can write

$$(\theta_s - \theta_0)\frac{c_s}{L\sqrt{\pi}} = \zeta e^{\zeta^2}\phi. \tag{2.61}$$

Then, adding equations (2.58) and (2.61), we get

$$\frac{(\theta_f - \theta_0)c_s}{L\sqrt{\pi}} = \zeta e^{\zeta^2}\,[\text{erf}\,(\zeta) + \phi]. \tag{2.62}$$

Now, the left-hand side and ϕ in equation (2.62) are known; so, ζ can be determined either graphically or by trial and error, as mentioned in Section 2.5.5. In the former approach, a graph of $\zeta e^{\zeta^2}\,[\text{erf}\,(\zeta) + \phi]$ versus ζ should be drawn for the given value of ϕ, and ζ can then be solved for with the known value of the left-hand side of equation (2.62). Once ζ is known, the depth of solidification can be computed from equation (2.47) and the solidification time from equation (2.52). For such a casting to be feasible, it should be ensured that θ_s works out to be less than the melting point of the mould metal.

EXAMPLE 2.6 Determine the solidification time of the slab-shaped casting considered in Example 2.5 when

(i) the casting is done in a water cooled copper mould,

(ii) the casting is made in a very thick copper mould.

In both cases, assume no resistance at the mould-metal interface and use the following data:

For iron	*For copper*
$c_s = 0.67$ kJ/kg-K	$c = 0.376$ kJ/kg-K
$k_s = 83$ W/m-K	$\rho = 8960$ kg/m^3
$\theta_f = 1540$°C	$k = 398$ W/m-K
$L = 272$ kJ/kg	
$\rho_m = 7850$ kg/m^3	

SOLUTION (i) In this case, $\theta_s = 28$°C and $h = 0.1$ m. So, from equation (2.51),

$$\zeta e^{\zeta^2} \operatorname{erf}(\zeta) = \frac{(1540 - 28) \times 0.67}{272\sqrt{\pi}} = 2.1$$

or

$$\zeta = 0.98.$$

Now,

$$\alpha_s = \frac{k_s}{\rho_m c_s} = \frac{83}{7850 \times 0.67 \times 10^3} \text{ m}^2/\text{sec}$$

$$= 15.8 \times 10^{-6} \text{ m}^2/\text{sec}.$$

The solidification time t_s is given by equation (2.52) as

$$t_s = \frac{(0.1)^2}{16 \times (0.98)^2 \times 15.8 \times 10^{-6}} \text{ sec} = 0.0115 \text{ hr}.$$

(ii) From the given data, using equation (2.60), we have

$$\phi = \left(\frac{83 \times 7850 \times 0.67}{398 \times 8960 \times 0.376}\right)^{1/2} = 0.57.$$

From equation (2.62) with $\theta_0 = 28$°C,

$$\zeta e^{\zeta^2}[\operatorname{erf}(\zeta) + 0.57] = \frac{(1540 - 28) \times 0.67}{272\sqrt{\pi}} = 2.1$$

or

$$\zeta = 0.815.$$

The solidification time, again from equation (2.52), is obtained as

$$t_s = \frac{(0.1)^2}{16 \times (0.815)^2 \times 15.8 \times 10^{-6}} \text{ sec} = 0.0165 \text{ hr}.$$

The surface temperature of the mould (θ_s) can be found from equation (2.58). Thus,

$$\frac{(1540 - \theta_s) \times 0.67}{272\sqrt{\pi}} = 0.815 e^{0.664} \operatorname{erf}(0.815)$$

$$= 0.815 \times 1.943 \times 0.75 = 1.188$$

or

$$\theta_s = (1540 - 854)\text{°C} = 685.4\text{°C}.$$

Since the melting point of copper is 1080°C, the mould will not melt away.

Comparing the solidification times obtained in Example 2.5 with those in Example 2.6, we find that the solidification time in the thick copper mould is almost twice that in the water cooled copper mould and both are of an order of magnitude less than that in the sand mould. Thus, the production rate in a metal mould is much higher than that in a sand mould.

In the foregoing analysis, the thermal resistance at the interface was totally neglected. However, in real practice, the mould wall expands due to heating and the casting surface shrinks due to cooling, resulting in a gap. Moreover, the wetting of the mould face by the liquid metal is never complete. All these facts suggest that a thermal resistance at the interface is inevitable. In what follows, we attempt to approximately account for the thermal resistance of layers 2, 3, 4 (Fig. 2.19). The temperature profile under such circumstances is as shown in Fig. 2.26. Here, two separate

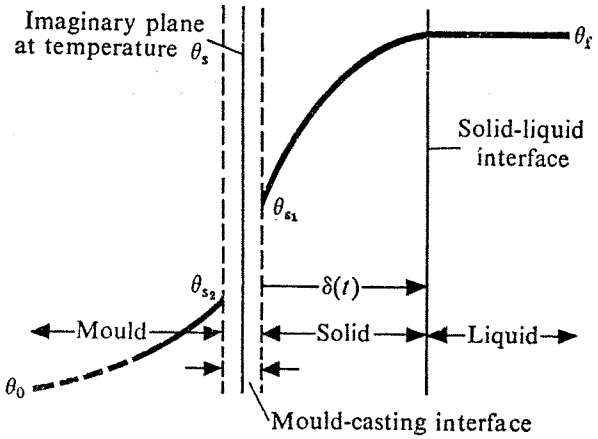

Fig. 2.26 Methodology for taking thermal resistance at mould-casting interface into consideration.

surfaces are imagined on either side of the interface, at temperatures θ_{s_1} (on the casting side) and θ_{s_2} (on the mould side). The film heat transfer coefficient h_f is apportioned on these two sides according to the equations

$$h_2 = (1 + \sqrt{\frac{k\rho c}{k_s\rho_m c_s}})h_f, \tag{2.63a}$$

$$h_1 = (1 + \sqrt{\frac{k_s\rho_m c_s}{k\rho c}})h_f. \tag{2.63b}$$

The temperature θ_s at the imaginary interface is calculated by neglecting the interface resistance (as done in Example 2.6). The solidification depth $\delta(t)$ can then be obtained as[1]

$$\delta(t) = \frac{h_1(\theta_f - \theta_s)}{\rho_m La}t - \frac{h_1}{2k_s}\delta^2(t), \tag{2.64}$$

where the factor a is given by the relation

$$a = \tfrac{1}{2} + \sqrt{\tfrac{1}{4} + \frac{c_s(\theta_f - \theta_s)}{3L}}. \tag{2.65}$$

Further, the solidification time t_s can be obtained from equation (2.64) with $\delta(t_s) = h/2$, h being the thickness of the slab. The mould surface temperature θ_{s_2}, when the casting has completely solidified, is given by[1]

$$\frac{\theta_{s_2} - \theta_0}{\theta_s - \theta_0} = 1 - e^{\gamma}[1 - \text{erf}\,(\sqrt{\gamma})], \tag{2.66}$$

where

$$\gamma = \frac{h_2^2}{k^2}\alpha t_s \tag{2.67}$$

and θ_0 is the initial temperature of the mould.

EXAMPLE 2.7 Estimate the solidification time and the mould surface temperature for the casting considered in Example 2.6(ii) with the total heat transfer coefficient across the casting-mould interface given as 1420 W/m²-°C.

SOLUTION From Example 2.6(ii), $\theta_s = 982$°C. Using equation (2.63b), we have

$$h_1 = [1 + \sqrt{\frac{83 \times 7850 \times 0.67}{398 \times 8960 \times 0.376}}]1420 \text{ W/m}^2\text{-°C}$$
$$= 2230 \text{ W/m}^2\text{-°C}.$$

[1]Geiger, G.H. and Poirier, D.R., Transport Phenomena in Metallurgy, Addison-Wesley, Reading, Massachusetts, 1973.

From equation (2.65),

$$a = \tfrac{1}{2} + \sqrt{\tfrac{1}{4} + \frac{0.67(1540 - 982)}{3 \times 272}} = 1.34.$$

Now, using equation (2.64) with $\delta(t_s) = h/2 = 0.05$ m, the solidification time t_s we obtain is

$$0.05 = \frac{2.230 \times (1540 - 982)}{7850 \times 272 \times 1.34}t_s - \frac{2230}{2 \times 83}(0.05)^2 \text{ sec}$$

or

$$t_s = 192.2 \text{ sec} \equiv 0.0533 \text{ hr}$$

which is significantly more than that estimated in Example 2.6(ii). To compute the mould surface temperature, we first calculate h_2, using equation (2.63a), as

$$h_2 = (1 + \sqrt{\frac{398 \times 8960 \times 0.376}{83 \times 7850 \times 0.67}}) \times 1420 \text{ W/m}^2\text{-°C} = 3909 \text{ W/m}^2\text{-°C}.$$

Now, from equation (2.67),

$$\gamma = \frac{3909 \times 3909}{398 \times 398}\frac{0.398 \times 192.2}{8960 \times 0.376} = 2.19.$$

So, using equation (2.66), the mould surface temperature θ_{s_2}, when the entire casting has solidified, we obtain is (with $\theta_0 = 28$°C and using the error function tables)

$$\theta_{s_2} = 28 + (982 - 28)[1 - 8.935(1 - 0.962)]\text{°C} = 658.1\text{°C}$$

which, again, is much less than the value of θ_s estimated in Example 2.6(ii).

2.5.7 CONTINUOUS CASTING PROCESS

Another situation where estimation of the solidification rate and heat transfer calculations are important is the continuous casting process. Here, no riser is used, and the casting is withdrawn continuously from one end of a water cooled mould while the liquid metal is fed continuously at the other end. Figure 2.27 schematically shows the continuous casting process. The heat transfer calculation in such a case is most conveniently represented by means of three nondimensional groups, namely[1],

$$\frac{h_f^2 y}{uk_s\rho_m c_s}, \quad \frac{L'}{c_s(\theta_f - \theta_0)}, \quad \frac{h_f\delta}{k_s},$$

where h_f is the film heat transfer coefficient at the mould-casting interface, y is the distance along the mould, u is the velocity of withdrawal of the

[1]Geiger, G.H. and Poirier, D.R., Transport Phenomena in Metallurgy, Addison-Wesley, Reading, Massachusetts, 1973.

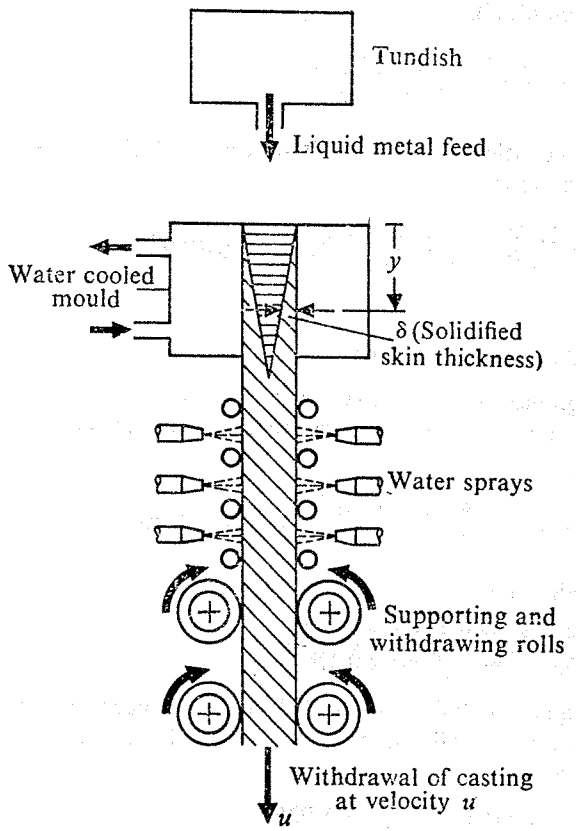

Fig. 2.27 Continuous casting process.

casting, θ_0 is the temperature of the water cooled mould, δ is the solidified skin thickness,

$$L' = L + c_m(\theta_p - \theta_f),$$

and all the other symbols are the same as used in the earlier sections. The results are presented in Figs. 2.28–2.30 in terms of these nondimensional parameters. These figures can be used for an estimation of important quantities such as the minimum mould length for a desired withdrawal rate, the skin depth of the casting, and the minimum cooling water flow rate for a maximum allowable temperature rise of the cooling water (see also the example that follows).

EXAMPLE 2.8 Determine (i) the mould length and (ii) the cooling water requirement to produce a continuous casting of steel slab with a cross-section of 60 cm × 7.5 cm at a withdrawal rate of 300 cm/min. The solid skin at the mould exit should be 1.25 cm thick and the film heat transfer

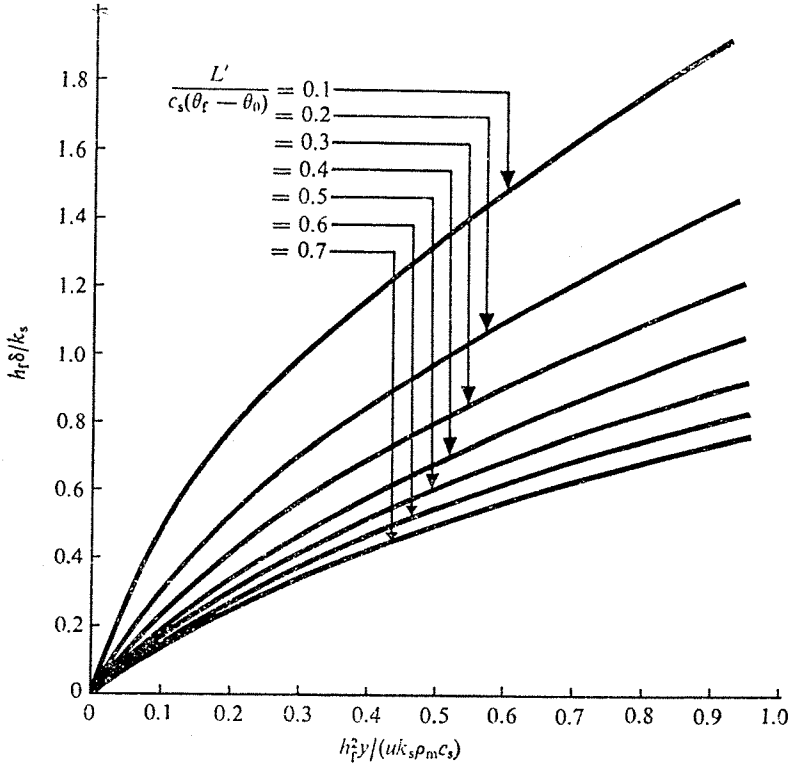

Fig. 2.28 Thickness solidified versus distance down the mould (after Hills, A.W.D. and Moore, M.R., Heat and Mass Transfer in Process Metallurgy, Institute of Mining and Metallurgy, London, 1967).

coefficient at the mould-casting interface is 1420 W/m²-°C. The temperature of the cooling water should not rise by more than 10°C. The mould is maintained at 20°C. The data for steel is

$$\theta_p = 1550°C, \quad \theta_f = 1500°C, \quad L = 268 \text{ kJ/kg},$$

$$\rho_m = 7680 \text{ kg/m}^3, \quad c_s = 0.67 \text{ kJ/kg-K}, \quad k_s = 76 \text{ W/m-K},$$

$$c_m = 0.755 \text{ kJ/kg-K}.$$

SOLUTION From the given data, we note that with $y = l_m$, the value of the skin thickness $\delta = 0.0125$ m, $u = 0.05$ m/sec, $\theta_0 = 20°C$, and

$$L' = 268 + 0.755 \times (1550 - 1500) \text{ kJ/kg} = 305 \text{ kJ/kg}.$$

So,

$$\frac{L'}{c_s(\theta_f - \theta_0)} = \frac{305}{0.67 \times 1480} = 0.308,$$

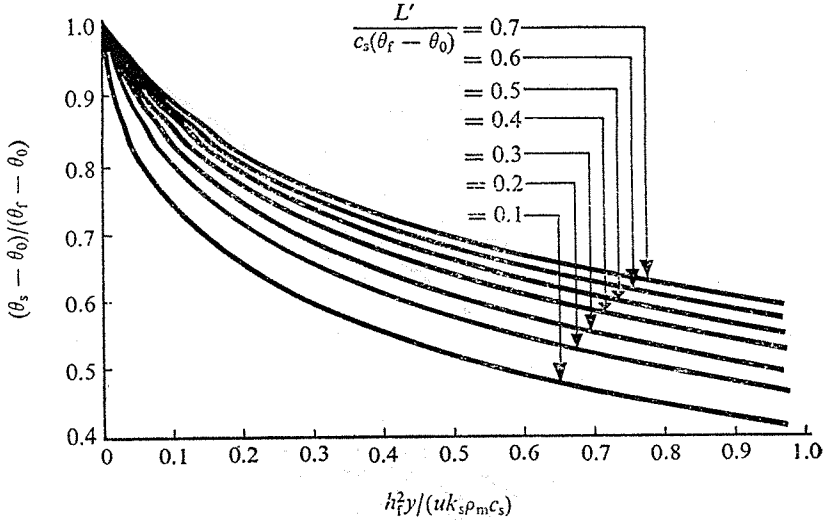

Fig. 2.29 Surface temperature versus distance down the mould (after Hills, A.W.D. and Moore, M.R., Heat and Mass Transfer in Process Metallurgy, Institute of Mining and Metallurgy, London, 1967).

$$\frac{h_f \delta}{k_s} = \frac{1420 \times 0.0125}{76} = 0.234.$$

From Fig. 2.28, for these values of the parameters (with $y = l_m$), we get

$$\frac{h_f^2 l_m}{uk_s\rho_m c_s} = 0.11.$$

Hence,

$$l_m = \frac{0.11 \times 0.05 \times 76 \times 7680 \times 670}{(1420)^2} = 1.07 \text{ m}.$$

Again, from Fig. 2.30,

$$\frac{Q}{l_m(\theta_f - \theta_0)\sqrt{l_m u \rho_m c_s k_s}} = 0.28 \quad \text{or} \quad Q = 2.12 \text{ MW}.$$

Hence, the cooling water requirement $\dot{m}$ is found out from the relation

$$\dot{m} c_w \Delta\theta = 2.12 \text{ MW} \qquad (\text{with } c_w = 4.2 \text{ kJ/kg}, \Delta\theta = 10°\text{C})$$

or

$$\dot{m} = \frac{2.12 \times 10^6}{4.2 \times 10^3 \times 10} \text{ kg/sec} = 5.05 \text{ kg/sec}.$$

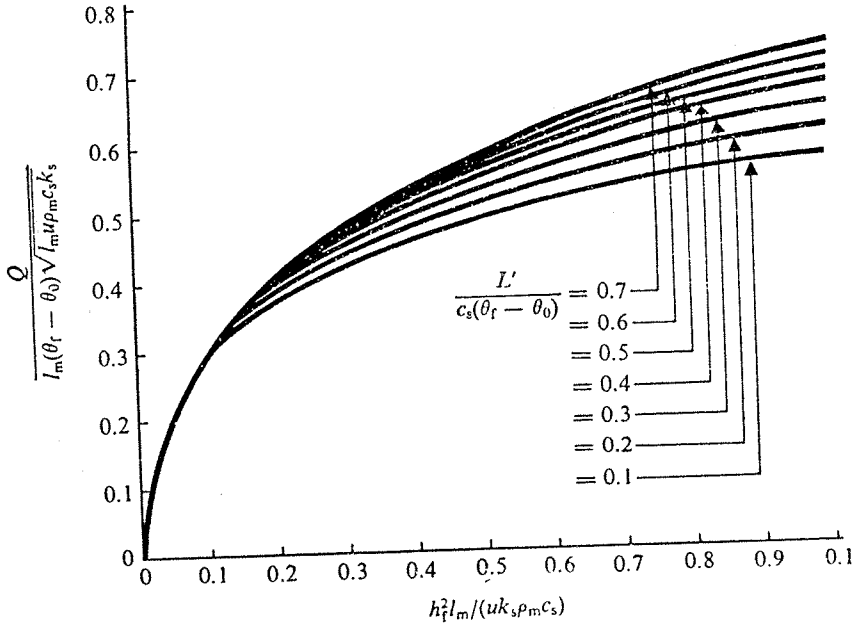

Fig. 2.30 Rate of heat removal by mould cooling water Q versus mould length l_m (after Hills, A.W.D. and Moore, M.R., Heat and Mass Transfer in Process Metallurgy, Institute of Mining and Metallurgy, London, 1967).

2.5.8 RISER DESIGN AND PLACEMENT

From the heat transfer analysis presented in Sections 2.5.5 and 2.5.6 we see that the solidification time depends primarily on the ratio V/A, where V is the volume of the casting and A is the surface area of heat dissipation (i.e., of the casting). This is also to be expected intuitively since the amount of heat content is proportional to volume and the rate of heat dissipation depends on the surface area. This information is utilized when designing a riser to ensure that the riser solidifies after the casting. However, the information on the amount of liquid metal needed from the riser is used only to compensate for the shrinkage that takes place from the pouring temperature till solidification. Depending on the metal, the percentage of this shrinkage varies from 2.5 to 7.5. Thus, the use of a large riser volume (to ensure large solidification time) is uneconomical. So, a riser should be designed with the minimum possible volume while maintaining a cooling rate slower than that of the casting.

It may be noted that a casting with a high surface area/volume ratio requires a riser larger than that determined by considering only the cooling rate. This is shown clearly by the example that follows.

Let us consider a steel plate of dimensions 25 cm × 25 cm × 0.25 cm. The casting then has the A/V ratio as

$$(\frac{A}{V})_c = \frac{2 \times 625 + 4(25 \times 0.25)}{25 \times 25 \times 0.25} \text{ cm}^{-1} = 8.16 \text{ cm}^{-1}.$$

A cubical riser with sides 1.25 cm has the A/V ratio as

$$(\frac{A}{V})_r = \frac{6 \times 1.25 \times 1.25}{1.25 \times 1.25 \times 1.25} = 4.8 \text{ cm}^{-1}.$$

Thus, the riser is assured to have a much slower cooling rate (more solidification time) than that of the casting. The volume shrinkage of steel during solidification is 3%. So, the minimum volume of the riser necessary is

$$0.03 \times \tfrac{625}{4} \text{ cm}^3 = 4.69 \text{ cm}^3.$$

The riser we have considered has the volume 1.95 cm³ only. Therefore, a much larger riser is required.

For a given shape of the riser, the dimensions of the riser should, however, be chosen so as to give a minimum A/V ratio, and the minimum volume should be ensured from the shrinkage consideration. It must be remembered that a liquid metal flows from the riser into the mould only during the early part of the solidification process. This necessitates the minimum volume of the riser to be approximately three times that dictated by the shrinkage consideration alone.

EXAMPLE 2.9 Determine the dimensions of a cylindrical riser to be used for casting as aluminium cube of sides 15 cm. The volume shrinkage of aluminium during solidification is 6.5%.

SOLUTION First of all, let us determine the diameter/height ratio of the most compact cylinder so that, for a given volume, the surface area is minimum. With the diameter and the height of the cylinder as d and h, respectively, the surface area of the cylinder is

$$A = \pi dh + 2\frac{\pi}{4}d^2$$

and the volume of the cylinder is

$$V = \frac{\pi}{4}d^2h \quad \text{or} \quad h = \frac{4V}{\pi d^2}.$$

Hence,

$$A = \pi d\frac{4V}{\pi d^2} + 2\frac{\pi}{4}d^2 = \frac{4V}{d} + \frac{\pi}{2}d^2.$$

For A to be minimum,

$$\frac{\partial A}{\partial d} = 0 \quad \text{or} \quad -\frac{4V}{d^2} + \pi d = 0 \quad \text{or} \quad d^3 = \frac{4V}{\pi}.$$

Again,

$$\frac{4V}{\pi} = d^2h = d^3$$

or

$$h = d^1 \qquad (\text{when } \frac{A}{V} = \frac{6}{d}).$$

Now, the minimum volume necessary for the riser is $V_r = 3 \times 0.065 V_c$, where V_c is the volume of the casting and is equal to 3375 cm³. So, $V_r = 658.2$ cm³. Thus, the diameter of the riser (d), which is also equal to the height of the riser, can be written as

$$h = (\frac{4V_r}{\pi})^{1/3} = 9.43 \text{ cm}.$$

Now,

$$(\frac{A}{V})_r = \frac{6}{d} = \frac{6}{h} = \frac{6}{9.43} \text{ cm}^{-1} = 0.636 \text{ cm}^{-1},$$

$$(\frac{A}{V})_c = \frac{6 \times 15 \times 15}{15^3} \text{ cm}^{-1} = 0.4 \text{ cm}^{-1} \qquad [\text{this is less than } (\frac{A}{V})_r].$$

So, the riser will not have a longer solidification time. The dimensions of the riser can be recalculated as follows. For

$$(\frac{A}{V})_r \leqslant (\frac{A}{V})_c,$$

we need

$$\frac{6}{d} \leqslant 0.4 \text{ cm}^{-1} \quad \text{or} \quad d \geqslant 15 \text{ cm}.$$

With the minimum value of d, $V_r = (\pi/4)d^2h = (\pi/4)d^3 = 2650$ cm³. This volume is much more than the minimum V_r necessary. Let us now consider the top riser when the optimum cylindrical shape is obtained with $h = d/2$ and again $(A/V)_r = 6/d$. However, with a large top riser, the cube loses its top surface for the purpose of heat dissipation. Hence,

$$(\frac{A}{V})_c = \frac{5 \times 15 \times 15}{15^3} \text{ cm}^{-1} = \tfrac{1}{3} \text{ cm}^{-1}.$$

To have

$$(\frac{A}{V})_r \leqslant (\frac{A}{V})_c \quad \text{or} \quad \frac{6}{d} \leqslant \tfrac{1}{3} \text{ cm}^{-1},$$

d should be greater than or equal to 18 cm. So, the riser volume with

[1]This optimum ratio $h/d = 1$ for a cylindrical riser is true only if the riser is attached to the side of the casting. For a riser attached to the top of a casting, the surface area $A = \pi dh + (\pi/4)d^2$ when the optimum ratio h/d turns out to be equal to 1/2. Sometimes, the dimensions to yield the minimum value of A for a given value of V are determined by using the Lagrange multiplier technique for constrained optimization (see Exercise 2.14).

minimum diameter is given as

$$V_r = \frac{\pi}{4}d^2h = \frac{\pi}{4}18^2 \times 9 \text{ cm}^3 = 2289 \text{ cm}^3$$

which is greater than the minimum V_r necessary. Though we see that with a top riser there is a little saving of material as compared with the side riser, we have to use, however, a deeper mould with the top riser. Thus, in this case, the side riser may be chosen.

To check the adequacy of the riser size for a steel casting, Caine's relationship is normally used. Equation (2.34) shows that the solidification time is proportional to the square of the ratio volume/surface area. Caine's relationship, however, is based on the assumption that the cooling rate is linearly proportional to the ratio surface area/volume. A typical risering curve is depicted in Fig. 2.31. Here, the ordinate of a point on the curve shows the

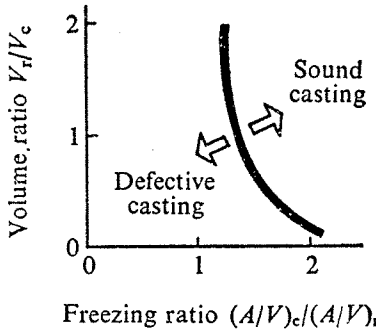

Fig. 2.31 Proper combinations of volume and freezing ratios.

volume ratio and the abscissa the freezing ratio; also, the subscripts c and r refer to the casting and the riser, respectively. For a given casting-riser combination, if the point in Fig. 2.31 falls to the right of the curve, the adequacy of the riser is ensured. The equation for a risering curve is of the form

$$x = \frac{a}{y - b} + c, \tag{2.68}$$

where a is the freezing constant for the metal, b is the contraction ratio from liquid to solid, and c is a constant depending on the different media around the riser and the casting. The value of c is unity if the mould material around the casting and the riser is the same. For steel, the typical values are $a = 0.1$ and $b = 0.03$.

The tedious calculation of $(A/V)_c$ for a complex casting has given rise to another method where a risering curve of the type shown in Fig. 2.32 is used. In this method, the shape factor $(l + w)/h$, instead of $(A/V)_c$, is plotted along the x-axis, where l, w, and h denote, respectively, the maximum length, the maximum width, and the maximum thickness of the casting. This method and Caine's relationship give almost identical results for a casting of simple

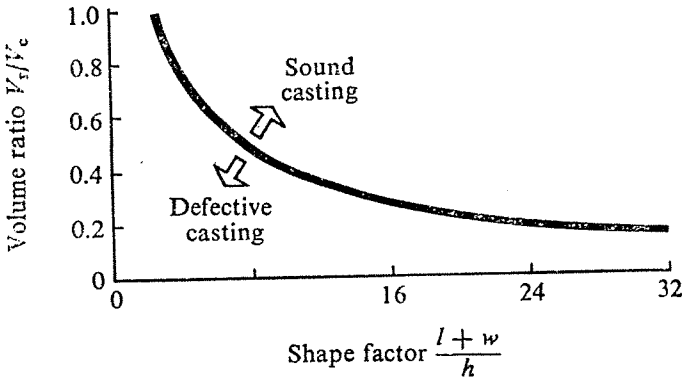

Fig. 2.32 Proper combinations of volume ratio and shape factor.

shape. If the appendages to the main body (of a simple, regular shape) of a casting are thin, then the solidification time does not alter significantly. As a result, a marginal increase in the calculated volume (on the basis of the main body) of the riser performs the job satisfactorily. As the appendages become heavier, the riser volume required is calculated on the basis of a modified total volume of the casting. The total volume of the casting is taken as the volume of the main section plus the effective percentage of the appendage volume, called the parasitic volume. The effective percentage is estimated from curves of the type shown in Fig. 2.33. A shape is called

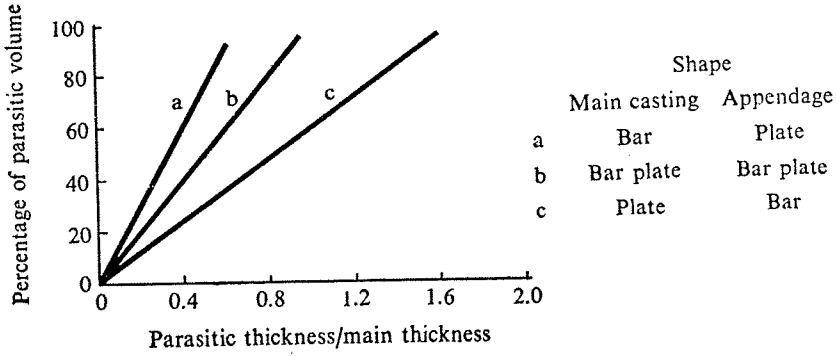

Fig. 2.33 Effective parasitic volume.

plate-like or *bar-like* depending on whether the width of the cross-section is more or less than three times the depth.

In the foregoing discussion, we assumed no special means of controlling the cooling rate (and hence the solidification time) of either the casting or of the riser. In practice, however, chill blocks (see Section 2.5.1) or thin fins are used on the casting to increase its cooling rate. Chilling is less effective for a

metal having a thermal conductivity higher than that of the chill. Similarly, to increase the solidification time of the riser, some exothermic compounds are added in the riser to keep it molten for a longer period.

So far, we have restricted our discussion to the adequacy of the riser size from the points of view of shrinkage and cooling rate. Another important aspect of risering is to ensure that the available liquid metal in the riser can be fed to the desired locations within the casting. For this, we should recall the concept of centre-line feeding resistance explained in Section 2.5.1.

In fact, the thermal gradient, within the casting, during the last stage of cooling is the most important factor. The minimum allowable gradient depends on the shape and size of the cross-section. Normally, for a casting with low (A/V) ratio (e.g., cube and sphere), one central riser is able to feed the entire casting. On the other hand, for a casting with high (A/V) ratio (e.g., for a bar and a plate), usually more than one riser is necessary. In such a case, a proper location of the riser has to be decided.

For a steel plate of up to 100 mm thickness, one central riser is satisfactory if the maximum feeding distance is less than 4.5 times the plate thickness. The feeding distance should be measured from the edge of the riser, as explained in Fig. 2.34a. It should be noted that, of the total distance $4.5t$, the riser gradient prevails up to a distance $2t$, whereas the end-wall gradient prevails in the remaining distance $2.5t$. Thus, the maximum distance between the edges of two consecutive risers is $4t$ and not $9t$ (see Fig. 2.34b).

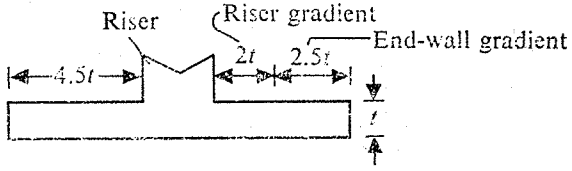

(a) Plate with one central riser

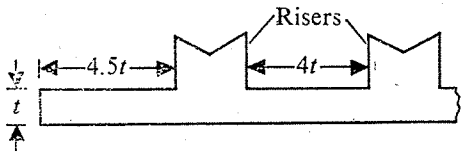

(b) Maximum distance between two consecutive risers

Fig. 2.34 Placement of risers.

A bar of square cross-section with sides measuring 50–200 mm can be fed satisfactorily from a single riser, up to a maximum distance of $30\sqrt{s}$, where s is the side of the square expressed in mm. The maximum distance between the edges of two consecutive risers is found to be $1.2s$ (and not $60\sqrt{s}$).

As mentioned in Section 2.5.1, the presence of a chill in the mould increases the feeding distance of the riser. This is achieved by providing a sharp thermal gradient with consequent decrease in the feeding resistance. It is obvious that the chill should be placed at the ends if a single riser is used. For more than one riser, the chill should be placed midway between the two risers. Figure 2.35 schematically explains the proper placement of risers and chills. The maximum permissible distances for various cases are also indicated in this figure.

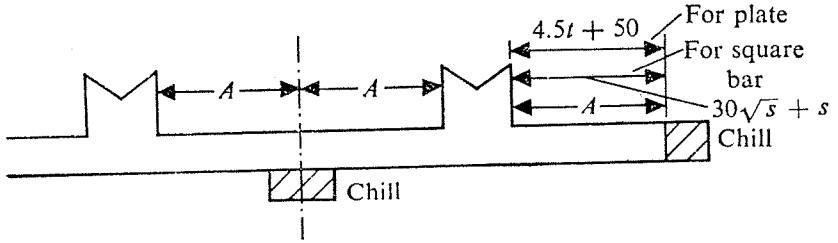

(All dimensions in mm)

Fig. 2.35 Placement of risers and chill blocks.

2.5.9 RESIDUAL STRESS

A sharp temperature gradient exists within a hot solidified casting of non-uniform cross-section. This is caused by the variation of heat content and the cross-sectional area available for its dissipation. This, in turn, results in varying amount of contraction in different parts of the casting, giving rise to high internal stresses. These (residual) stresses, if not properly controlled, may even cause tearing or cracking of the casting. A controlled cooling is therefore necessary to avoid high values of residual internal stresses. The method of control depends on various factors, e.g., material and shape of the casting. We shall now consider a typical example of a big cast iron car wheel.

Figure 2.36 shows the cross-section of the casting we are considering.

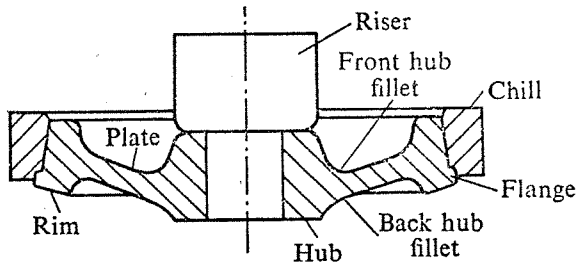

Fig. 2.36 Cross-section of wheel.

The cooling rate of the heavier rim is improved considerably by providing a chill. As a result, the temperature measurements, shortly after the solidi-

fication, show that the hub temperature is 930°C, the plate temperature is 760°C, and the tread temperature is 730°C. If the casting is left in the mould or is air cooled, the same trend of temperature variation continues. Ultimately, the final casting has a compressive circumferential stress in the tread of magnitude 70.7 N/mm^2 and a radial tensile stress at the front hub fillet measuring 222 N/mm^2. Such huge internal stresses can be avoided by taking out the casting at an average temperature of 760°C and putting it in an insulated pit when the cooling rate is brought down to 5.5°C/hr. The entire cooling takes about three days. At such a low cooling rate, temperature equalization takes place above 540°C. Any temperature gradient existing within the casting above this temperature does not give rise to elastic strain. In the temperature range exceeding 540°C, the elastic strain is relaxed to the plastic strain due to the high rate of creep. This avoids the development of high internal residual stresses. The stresses are found to be compressive, both in the tread (circumferential 8 N/mm^2) and in the fillet (radial 4 N/mm^2). If high internal residual stresses do exist in a casting, these should be taken care of either by subsequent heat treatment or by the other methods of stress relieving.

2.6 DEFECTS IN CASTINGS

In this section, we shall discuss the different types of defects in castings, and their origin and remedies. The treatment is restricted essentially to the sand mould castings. The defects in a casting may arise due to the defects in one or more of the following:

(i) Design of casting and pattern.

(ii) Moulding sand and design of mould and core.

(iii) Metal composition.

(iv) Melting and pouring.

(v) Gating and risering.

The following defects are most commonly encountered in the sand mould castings (Fig. 2.37):

(i) *Blow* It is a fairly large, well-rounded cavity produced by the gases which displace the molten metal at the cope surface of a casting. Blows usually occur on a convex casting surface and can be avoided by having a proper venting and an adequate permeability. A controlled content of moisture and volatile constituents in the sand-mix also helps in avoiding the blow holes.

(ii) *Scar* A shallow blow, usually found on a flat casting surface, is referred to as a scar.

(iii) *Blister* This is a scar covered by the thin layers of a metal.

(iv) *Gas holes* These refer to the entrapped gas bubbles having a nearly spherical shape, and occur when an excessive amount of gases is dissolved in the liquid metal.

(v) *Pin holes* These are nothing but tiny blow holes, and occur either

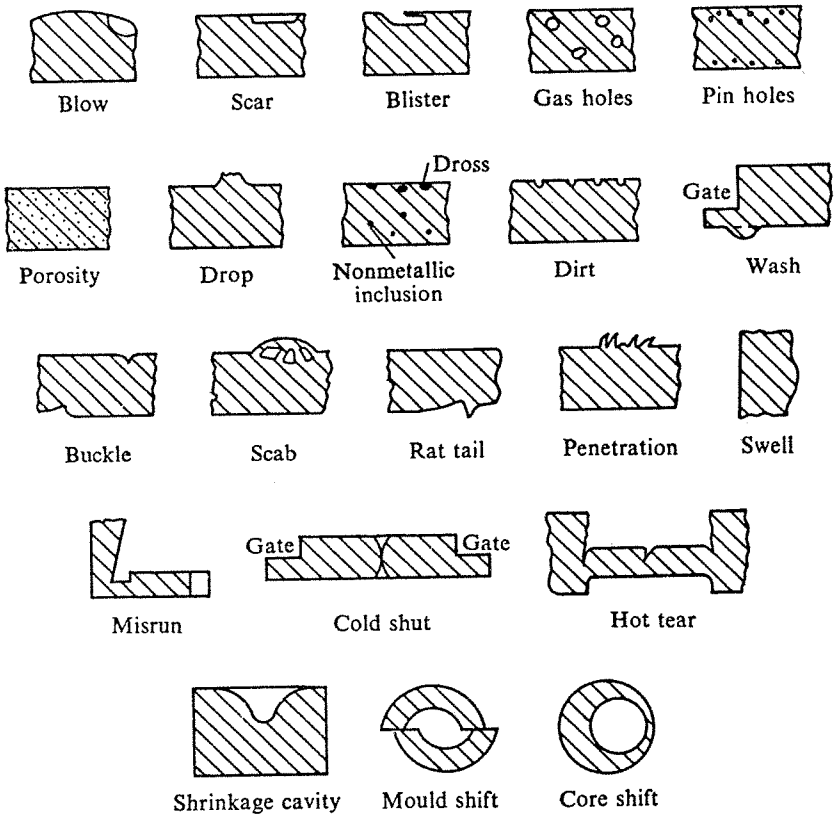

Fig. 2.37 Common casting defects.

at or just below the casting surface. Normally, these are found in large numbers and are almost uniformly distributed in the entire casting surface.

(vi) *Porosity* This indicates very small holes uniformly dispersed throughout a casting. It arises when there is a decrease in gas solubility during solidification.

(vii) *Drop* An irregularly-shaped projection on the cope surface of a casting is called a drop. This is caused by dropping of sand from the cope or other overhanging projections into the mould. An adequate strength of the sand and the use of gaggers can help in avoiding the drops.

(viii) *Inclusion* It refers to a nonmetallic particle in the metal matrix. It becomes highly undesirable when segregated.

(ix) *Dross* Lighter impurities appearing on the top surface of a casting are called dross. It can be taken care of at the pouring stage by using items such as a strainer and a skim bob.

(x) *Dirt* Sometimes sand particles dropping out of the cope get embedded on the top surface of a casting. When removed, these leave small,

angular holes, known as dirts. Defects such as drop and dirt suggest that a well-designed pattern should have as little a part as possible in the cope. Also, the most critical surface should be placed in the drag.

(xi) *Wash* A low projection on the drag surface of a casting commencing near the gate is called a wash. This is caused by the erosion of sand due to the high velocity jet of liquid metal in bottom gating.

(xii) *Buckle* This refers to a long, fairly shallow, broad, vee-shaped depression occurring in the surface of a flat casting of a high temperature metal. At this high temperature, an expansion of the thin layer of sand at the mould face takes place before the liquid metal at the mould face solidifies. As this expansion is obstructed by the flask, the mould face tends to bulge out, forming the vee shape. A proper amount of volatile additives in the sand-mix is therefore essential to make room for this expansion and to avoid the buckles.

(xiii) *Scab* This refers to the rough, thin layer of a metal, protruding above the casting surface, on top of a thin layer of sand. The layer is held on to the casting by a metal stringer through the sand. A scab results when the upheaved sand is separated from the mould surface and the liquid metal flows into the space between the mould and the displaced sand.

(xiv) *Rat tail* It is a long, shallow, angular depression normally found in a thin casting. The reason for its formation is the same as that for a buckle. Here, instead of the expanding sand upheaving, the compressed layer fails by one layer, gliding over the other.

(xv) *Penetration* If the mould surface is too soft and porous, the liquid metal may flow between the sand particles up to a distance, into the mould. This causes rough, porous projections and this defect is called penetration. The fusion of sand on a casting surface produces a rough, glossy appearance.

(xvi) *Swell* This defect is found on the vertical surfaces of a casting if the moulding sand is deformed by the hydrostatic pressure caused by the high moisture content in the sand.

(xvii) *Misrun* Many a time, the liquid metal may, due to insufficient superheat, start freezing before reaching the farthest point of the mould cavity. The defect that thus results is termed as a misrun.

(xviii) *Cold shut* For a casting with gates at its two sides, the misrun may show up at the centre of the casting. When this happens, the defect is called a cold shut.

(xix) *Hot tear* A crack that develops in a casting due to high residual stresses is called a hot tear.

(xx) *Shrinkage cavity* An improper riser may give rise to a defect called shrinkage cavity, as already detailed.

(xxi) *Shift* A misalignment between two halves of a mould or of a core may give rise to a defective casting, as shown in Fig. 2.37. Accordingly, this defect is called a mould shift or a core shift.

2.7 MISCELLANEOUS CASTING PROCESSES

We have so far discussed the basic features of the casting processes mainly with reference to the most common type of green sand mould casting. In this section, we shall briefly consider the other types of casting processes.

2.7.1 DRY SAND MOULD CASTING

The dry sand mould casting uses expendable moulds, i.e., each mould is used only once. A dry sand mould is basically a green sand mould baked in an oven at 100–250°C for several hours. The sand-mix contains 1–2% of pitch. The oxidation and polymerization of pitch increases the hot strength of the mould. As the water is driven out from the sand-mix by heating, the defects caused by the generation of steam, e.g., blows and porosity, are less frequent in dry sand mould casting.

2.7.2 SHELL MOULD CASTING

The shell mould casting is a semiprecise method for producing small castings repetitively in large numbers. The mould material contains phenolic resin mixed with fine, dry silica. These are mixed either dry or in the presence of alcohol; no water is used. Normally, a machined pattern of gray iron, aluminium, or brass is used in this process. First, the pattern is heated to 230–260°C, and then the sand-resin mixture is either dumped or blown over its surface. This way, the heated pattern melts and hardens the resin which, in turn, bonds the sand grains closely together. After a dwell time of 20–30 sec, the pattern and sand are inverted. When this happens, a layer of sand adheres to the pattern in the form of a shell of about 6 mm thickness. The rest of the sand is cleaned off. The thickness of the shell can be accurately controlled by controlling the dwell time. The thickness of the shell is so decided that the shell has the required strength and rigidity to hold the weight of the liquid metal to be poured into the mould. Then the mould is heated in an oven (at 300°C) for 15–60 sec. This curing makes the shell rigid when it can be stripped off by means of ejector pins mounted on the pattern. The shell thus formed constitutes one-half of the mould. Two such halves, placed one over the other, make the complete mould. While pouring the liquid metal, the two halves are clamped down together by clamps or springs.

It should be noted that in this process, the smoothness of the mould wall is independent of the moulder's skill. This contributes to a better dimensional accuracy and consistency when compared with green sand moulding. Smooth mould walls also offer less resistance to the flow of liquid metal in the mould. This is why smaller gates can be used. Moreover, thin sections, sharp corners, small projections, which are not possible in green sand moulds, can be accommodated. Further, subsequent machining operations are also reduced. Often, only grinding can produce the finished product. The increased cost of the metal pattern (as compared

with the wooden pattern used in green sand moulding), however, can be justified only if the casting is produced in large enough numbers.

2.7.3 INVESTMENT CASTING

The process of investment casting is suitable for casting a wide range of shapes and contours in small-size parts, especially those that are made of hard-to-machine materials. The process produces excellent surface finish for the casting. Here, the mould is made in a single piece, and consequently there is no parting line to leave out fins. This also adds to the dimensional accuracy of the casting. As will be apparent from the description of the process, no complication arises when withdrawing a pattern from the mould. Though the process is elaborate and expensive, it has been found very suitable for casting turbine and jet engine parts made of high temperature and high strength alloys. We now describe the steps to be followed in this process.

A rather accurately dimensioned metal pattern is used. The dimensions of the pattern are calculated to compensate for the several size adjustments which take place in the process—in the die, in the wax, in the investment material, and, finally, in the casting material. The determination of the pattern dimensions is a tedious task and requires considerable experimentation. This makes the pattern in an investment casting very costly.

This pattern is used to make a die out of a soft material, e.g., aluminium. Thereafter, wax or plastic is injected into the die to form an expendable pattern. The expendable pattern is rinsed in alcohol to remove grease and dirt. After drying, the pattern is dipped in a slurry composed of silica flour, water, and some bonding agent. Then, the pattern is taken out of the slurry and rotated to produce a uniform coating, to fill inside corners and to drain out the excess slurry. Sometimes, a number of expendable patterns are assembled as a 'tree' for economy. Finally, fine-grain silica sand is sprinkled onto the wet slurry surface. The coating thus produced on the expendable pattern after drying is called a precoat.

The pattern with the precoat is then placed on a steel base and is covered by an open-ended steel can. Both the pattern and the can are secured to the base by molten wax. Then, the can is filled with a slurry of heavy, self-hardening refractory concentrate. The concentrate sets in after a lapse of 24 hours when the can is placed in an oven. Thus, most of the wax or plastic melts and flows out of the mould, leaving a cavity with the shape of the intended casting. The residual wax is removed by firing the mould in a furnace for about 24 hours.

The liquid metal is poured into this mould while it is still hot. This saves the liquid metal from acquiring the moisture and avoids high thermal gradient between the liquid metal and the mould. In critical cases, the pouring is conducted in a vacuum chamber or in a protective inert atmosphere (such as argon). Frequently, the mould is clamped to a special type of furnace which is then inverted for pouring directly from the furnace into the mould. After cooling, the can is removed and the hard refractory investment is knocked off by a hammer or other vibratory means. Finally, the adhered investment material is removed from the casting surface by sand-blasting or a tumbling operation.

2.7.4 GRAVITY DIE CASTING

In gravity die casting, a permanent mould is used. The liquid metal is poured into a non-expendable mould under the force of gravity. The process is normally used for cast iron and, occasionally, for a nonferrous casting. The mould is made of heat resistant cast iron, and is provided with fins on its outer surface for efficient air-cooling. The inner surface of the mould cavity is sprayed with an oil-carbon-silica mixture before each pouring.

2.7.5 DIE CASTING

In the die casting process, unlike in gravity casting, the liquid metal is forced into the mould cavity under high pressure. The process is used for casting a low melting temperature material, e.g., aluminium and zinc alloys. The mould, normally called a die, is made in two halves (see Figs. 2.38–2.40), of which one is fixed and the other moving. Medium carbon, low alloy tool steel is the most common die material. The die is cooled by water for an efficient cooling of the casting. This also increases the die life. The process

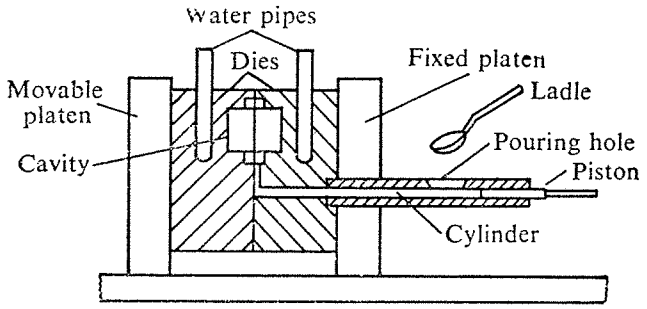

Fig. 2.38 Cold chamber.

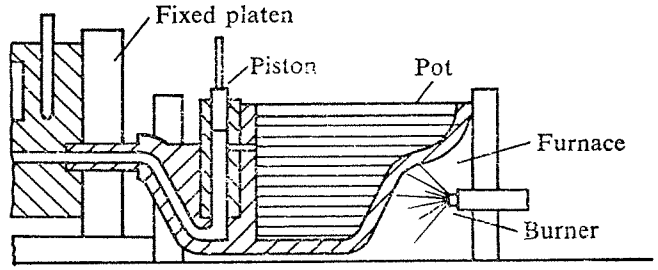

Fig. 2.39 Hot chamber.

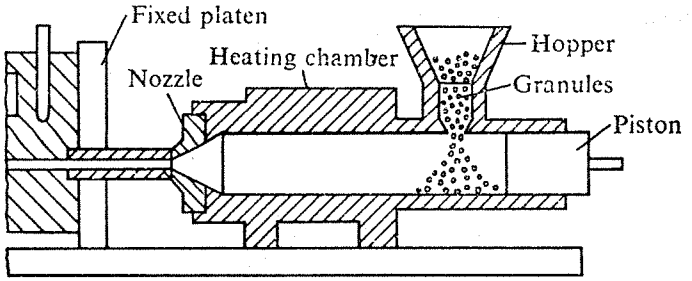

Fig. 2.40 Injection moulding.

is referred to as a hot chamber (Fig. 2.39) or a cold chamber (Fig. 2.38) process, depending on whether or not the melting furnace is an integral part of the mould. Since the liquid metal is forced into the die with high external pressure, much thinner sections can be cast by this process. The process, when applied to a plastic casting, is called injection moulding (Fig. 2.40).

2.7.6 CENTRIFUGAL CASTING

The centrifugal casting process is normally carried out in a permanent mould which is rotated during the solidification of a casting (Fig. 2.41). For producing a hollow part, the axis of rotation is placed at the centre of the desired casting. The speed of rotation is maintained high so as to produce a centripetal acceleration of the order of 60*g* to 75*g*. The centrifuge action segregates the less dense nonmetallic inclusions near the centre of rotation.

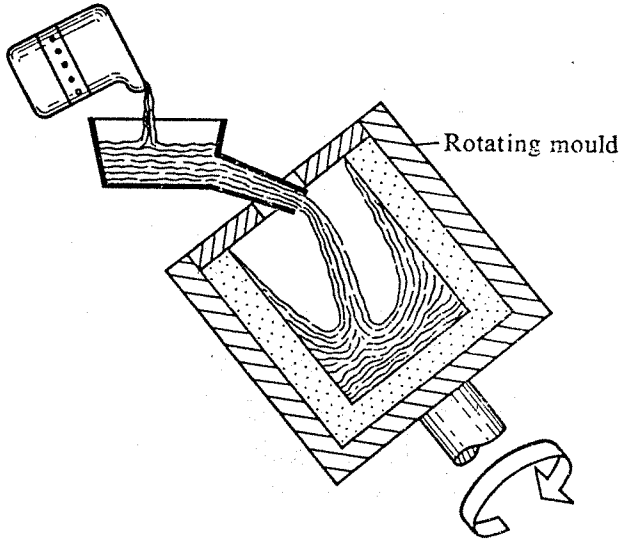

Fig. 2.41 Centrifugal casting.

It should be noted that the casting of hollow parts needs no core in this process. Solid parts can also be cast by this process by placing the entire mould cavity on one side of the axis of rotation. The castings, produced by this method, are obviously very dense. By having several mould cavities, more than one casting can be made simultaneously.

2.7.7 SLUSH CASTING

A slush casting is produced by pouring the liquid material into an open-top permanent mould and inverting the mould after a thin layer of the liquid has solidified on its surfaces. Thus, the liquid at the centre of the mould is drained out. The process results in shell-like castings which are widely used for ornamental objects, e.g., lamp shades and toys. Normally, low temperature materials such as tin, lead, and zinc are used in this process.

2.7.8 CO_2 PROCESS

The CO_2 process is essentially a sand moulding process where the sand-mix does not contain any oil, resin, or clay as the bonding agent. This eliminates the use of driers and the heating cycle. Instead, the sand-mix contains 2–6% of sodium silicate solution. This sand-mix has a very high flowability to fill up corners and intricate contours. The sand is hardened by passing CO_2 for about one minute. The CO_2 gas forms a weak acid that hydrolyzes the sodium silicate (Na_2O, SiO_2) solution to form amorphous silica which acts as the bond. Sodium silicate itself also provides some bonding action.

2.8 INSPECTION OF CASTINGS

Nondestructive inspection techniques are essential for creating a confidence when using a cast product. In this section, we shall briefly outline some of these techniques for testing the various kinds of defects.

Visual Inspection

Common defects such as rough surfaces (fused sand), obvious shifts, omission of cores, and surface cracks can be detected by a visual inspection of the casting. Cracks may also be detected by hitting the casting with a mallet and listening to the quality of the tone.

Pressure Test

The pressure test is conducted on a casting to be used as a pressure vessel. In this, first all the flanges and ports are blocked. Then, the casting is filled with water, oil, or compressed air. Thereafter, the casting is submerged in a soap solution when any leak will be evident by the bubbles that come out.

Magnetic Particle Inspection

The magnetic particle test is conducted to check for very small voids and cracks at or just below the surface of a casting of a ferromagnetic material.

The test involves inducing a magnetic field through the section under inspection. This done, the powdered ferromagnetic material is spread out onto the surface. The presence of voids or cracks in the section results in an abrupt change in the permeability of the surface; this, in turn, causes a leakage in the magnetic field. The powdered particles offer a low resistance path to the leakage. Thus, the particles accumulate on the disrupted magnetic field, outlining the boundary of a discontinuity.

Dye-Penetrant Inspection

The dye-penetrant method is used to detect invisible surface defects in a nonmagnetic casting. The casting is brushed with, sprayed with, or dipped into a dye containing a fluorescent material. The surface to be inspected is then wiped, dried, and viewed in darkness. The discontinuities in the surface will then be readily discernible.

Radiographic Examination

The radiographic method is expensive and is used only for subsurface exploration. In this, both X- and γ-rays are used. With γ-rays, more than one film can be exposed simultaneously; however, X-ray pictures are more distinct. Various defects, e.g., voids, nonmetallic inclusions, porosity, cracks, and tears, can be detected by this method. On the exposed film, the defects, being less dense, appear darker in contrast to the surrounding.

Ultrasonic Inspection

In the ultrasonic method, an oscillator is used to send an ultrasonic signal through the casting. Such a signal is readily transmitted through a homogeneous medium. However, on encountering a discontinuity, the signal is reflected back. This reflected signal is then detected by an ultrasonic detector. The time interval between sending the signal and receiving its reflection determines the location of the discontinuity. The method is not very suitable for a material with a high damping capacity (e.g., cast iron) because in such a case the signal gets considerably weakened over some distance.

2.9 EXERCISE PROBLEMS

2.1 Sketch the patterns with allowances for casting the following articles: (i) cast iron bearing block (Fig. 2.42a), (ii) aluminium bracket (Fig. 2.42b).

2.2 The grain size distribution of two samples of green sand for moulding is shown in Fig. 2.43. Which mould will have the higher permeability? Justify your answer.

2.3 In order to remove hydrogen from a liquid melt of iron of mass 100 kg, carbon monoxide bubbles are used so that the partial pressure of hydrogen falls to 0.1 atm. Determine the total volume of hydrogen in the liquid.

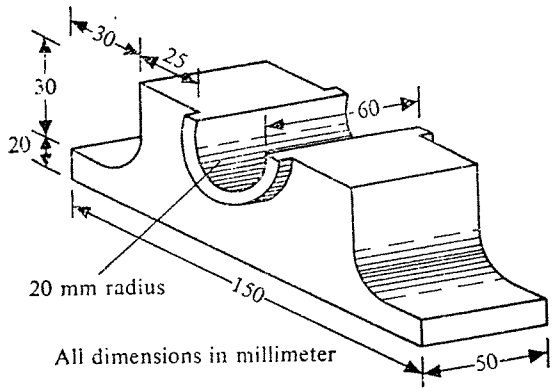

(a) Cast iron bearing block

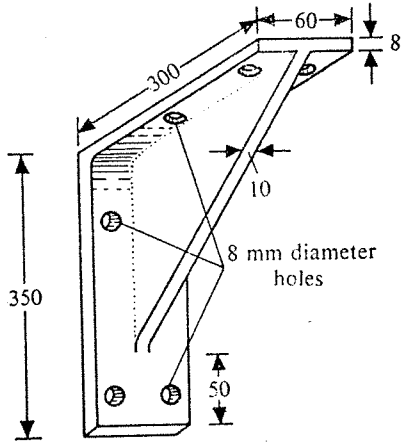

All dimensions in millimeter

(b) Aluminium bracket

Fig. 2.42 Jobs of Exercise 2.1.

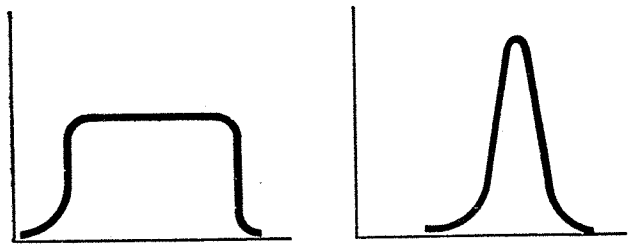

Fig. 2.43 Grain size distribution.

2.4 Figure 2.44 shows a mould along with the riser for casting a plate 20 cm × 20 cm × 5 cm. Determine the area A_g such that the mould and the riser get filled up within 10 sec after the downsprue has been filled. It should be noted that $A_3 \gg A_g$ since below the downsprue a flat gate is attached to the casting. Neglect the frictional and orifice effects.

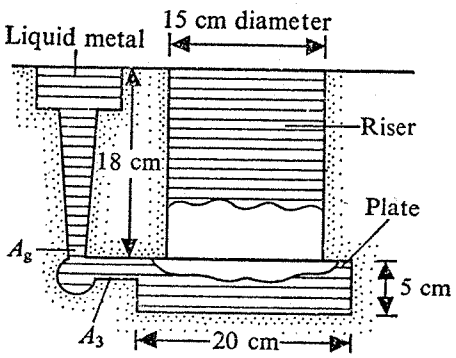

Fig. 2.44 Mould for casting plate.

2.5 Design the downsprue, avoiding aspiration, shown in Fig. 2.45 to deliver liquid cast iron ($\rho_m = 7800$ kg/m^3) at a rate of 10 kg/sec against no head at the base of the sprue. Neglect the frictional and orifice effects.

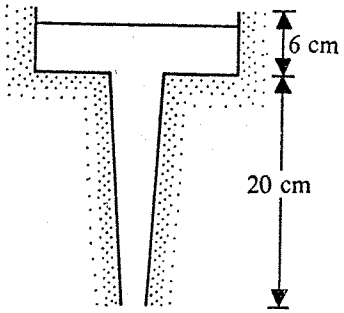

Fig. 2.45 Downsprue for delivering liquid cast iron.

2.6 Figure 2.46 shows the casting of a seamless metal pipe in a cooled mould. A pressure pouring technique is used to fill the mould quickly, as depicted in the figure. Determine the expression for estimating the time taken to fill up only the mould. Assume that the level h_1 in the ladle does not change. You may neglect the frictional losses but not the entrance losses.

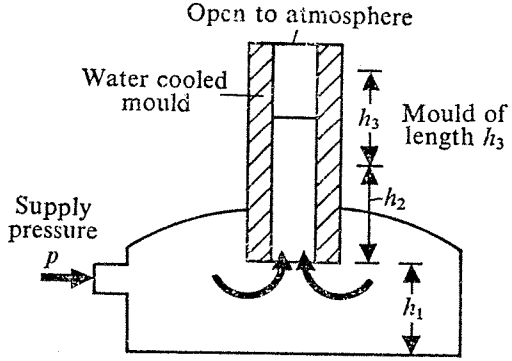

Fig. 2.46 Pressure pouring technique.

2.7 A ladle containing molten steel is placed in a pressurized chamber (Fig. 2.47). The air pressure in the chamber is increased to 0.3 N/mm^2 in order to force the molten metal into the mould through the pouring tube. Estimate the time taken to fill up the mould. Also, account for the frictional losses in the tube and the losses due to sudden contraction and expansion.

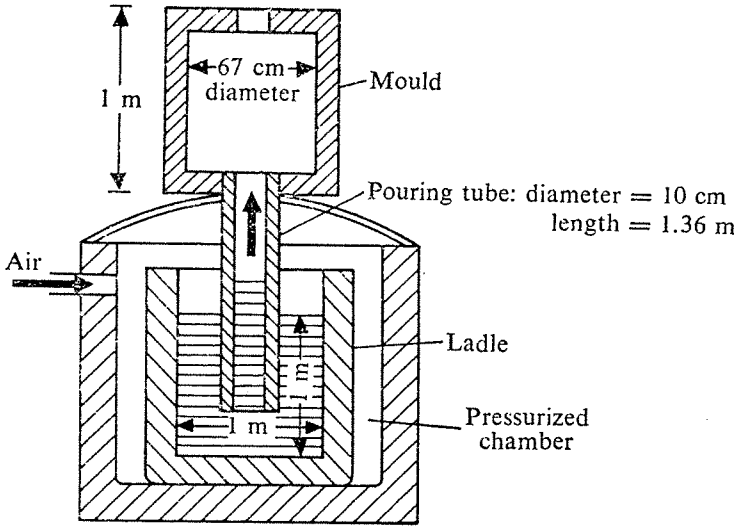

Fig. 2.47 Filling up mould using pressurized chamber.

Initially, half of the tube length is submerged into the melt. For steel, $\rho_m = 7600$ kg/m^3, and $\eta = 0.00595$ kg/m-sec.

2.8 Estimate the time to fill up the mould shown in Fig. 2.48. Assume that the liquid metal level at X-X is maintained constant and the time to fill the runner is negligible. The following data can all be treated as

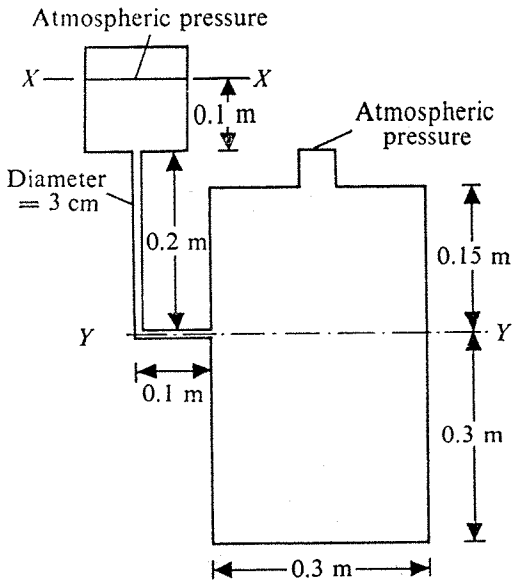

Fig. 2.48 System of Problem 2.8.

constants:

$\rho_m = 6000$ kg/m^3, $\eta = 0.00165$ kg/m-sec, f(runner) $= 0.0025$,

e_f (contraction) $= 0.1$, $\beta = 1.0$, $(L/D)_{eq}$ for 90° turn $= 25$,

e_f (enlargement for levels below Y-Y) $= 0$,

e_f (enlargement for levels above Y-Y) $= 1.0$.

2.9 A continuous casting operation is illustrated in Fig. 2.49. The liquid level in the tundish and the degasser is maintained at the height indicated in the figure. Determine the tundish and degasser nozzle sizes for a production rate of 25,000 kg/hr per strand. The given data are

$\rho_m = 7600$ kg/m^3,

discharge coefficient for each nozzle $= 0.8$,

vacuum pressure $= 10^{-3}$ atm.

2.10 Is it possible to cast an iron slab, poured at its melting point, in a very thick aluminium mould? Justify your answer quantitatively. Assume no thermal resistance at the mould-metal interface. Use the following data:

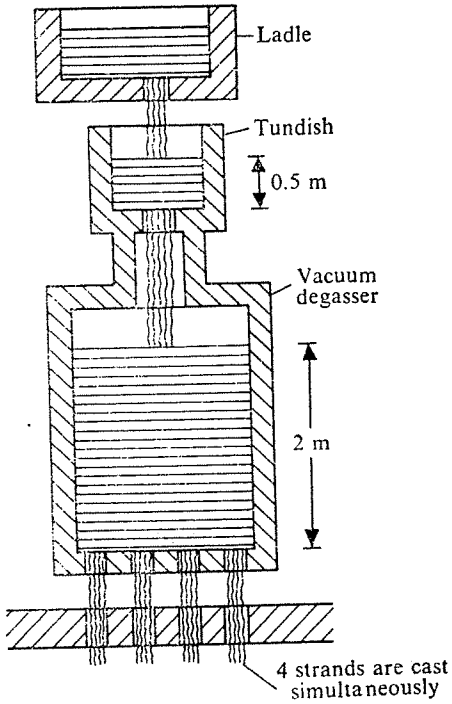

Fig. 2.49 Continuous casting with degasser.

For iron	*For aluminium*
$c = 0.67$ kJ/kg-K	$c = 1.12$ kJ/kg-K
$k = 83$ W/m-K	$k = 498$ W/m-K
$\rho = 7850$ kg/m^3	$\rho = 2748$ kg/m^3
$L = 272$ kJ/kg	room temperature = 28°C
melting point = 1540°C	melting point = 660°C

2.11 Estimate the surface temperature of a sand mould while casting iron, poured at its melting point, using the analysis given in Section 2.5.6, and hence justify the assumption $\theta_s = \theta_f$ made in Section 2.5.3. Use the property values given in Example 2.5 and Exercise 2.10.

2.12 While casting an L-section, a shrinkage cavity is formed, as shown in Fig. 2.50a. Explain physically why the formation of a shrinkage cavity should be avoided in situations of the type shown in Figs. 2.50b and 2.50c.

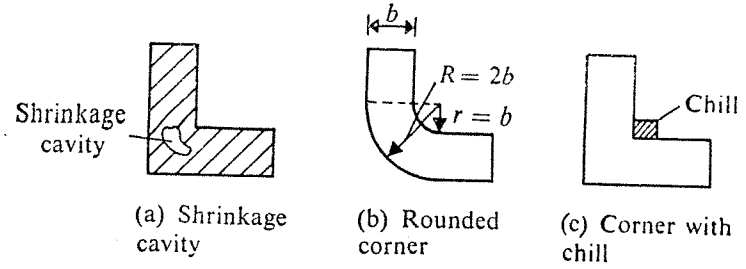

(a) Shrinkage cavity (b) Rounded corner (c) Corner with chill

Fig. 2.50 Development of shrinkage cavity and means of avoiding it.

2.13 Slab-shaped steel castings, made in sand moulds, show centre-line porosity due to a meeting of the two solidification fronts, as explained in Fig. 2.51a. The solidification time of a 5-cm-thick steel casting in a sand mould is found to be 6 min. The same casting takes 60 min to solidify when placed in an insulating mullite mould. If the casting is made in a composite mould, as sketched in Fig. 2.51b, determine the thickness d to be cast such that, after machining, a 47-mm-thick, sound casting is obtained.
[*Hint* The machining allowance for cast steel is 3 mm (see Table 2.1) for the dimension given. Hence, $d_1 = 47 + 3 = 50$ mm.]

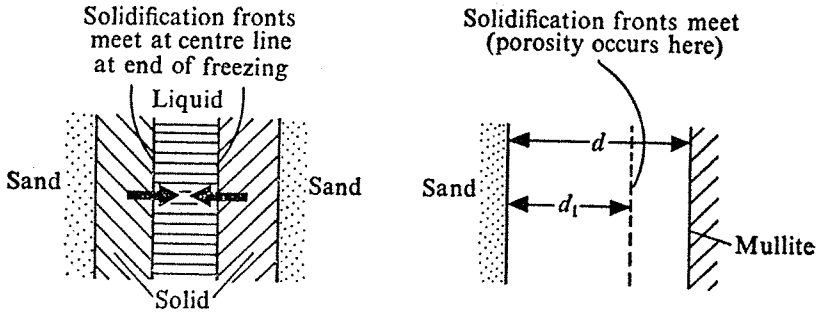

(a) Symmetrical mould (b) Composite mould

Fig. 2.51 Solidification front in symmetrical and composite moulds.

2.14 Compare the solidification time of two *optimum* risers of the same volume when one has a cylindrical shape and the other is of the form of a rectangular parallelopiped.

2.15 Determine the dimensions of an optimum cylindrical riser attached to the side of a steel plate casting having the dimensions 25 cm × 12.5 cm × 5 cm by

(i) using Caine's relationship, i.e., equation (2.68),
(ii) using Fig. 2.32,
(iii) assuming that the volume shrinkage on solidification is 3% for steel

and that the volume of the riser is three times that dictated by the shrinkage consideration alone.

2.16 Estimate the riser volume necessary if a bar of cross-section 2.5 cm × 2.5 cm and 10 cm long is added to the plate considered in Exercise 2.15.

2.17 Design an economic risering system for the steel casting shown in Fig. 2.52, taking into account the problem of feeding distance.

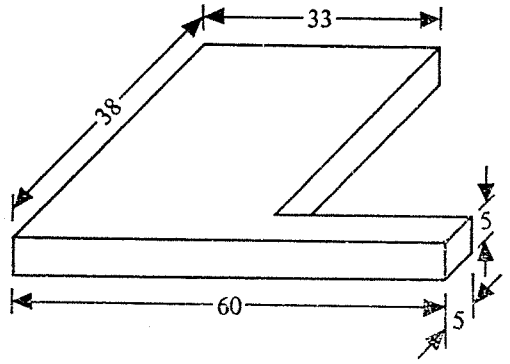

All dimensions in millimeter

Fig. 2.52 Steel casting.